Journal of Hydrology (2008) 352, 267–287

available at www.sciencedirect.com

ScienceDirect

journal homepage: www.elsevier.com/locate/jhydrol

Application of multiple isotopic and geochemical tracers for investigation of recharge, salinization, and residence time of water in the Souss–Massa aquifer, southwest of Morocco

L. Bouchaou [a,*], J.L. Michelot [b], A. Vengosh [c], Y. Hsissou [a], M. Qurtobi [d], C.B. Gaye [e,1], T.D. Bullen [f], G.M. Zuppi [g]

[a] *Laboratoire de Géologie Appliquée et Géo-Environnement, Université Ibn Zohr, Faculté des Sciences, B.P. 8106, 80000 Agadir, Morocco*
[b] *UMR ''IDES'', CNRS – Université Paris-Sud, Orsay, France*
[c] *Division of Earth and Ocean Sciences, Nicholas School of Environment and Earth Sciences, Duke University, Durham, NC, USA*
[d] *Centre National de l'Energie des Sciences et des Techniques Nucléaires (CNESTEN), Rabat, Morocco*
[e] *Université Cheikh Anta Diop Dakar, Senegal*
[f] *US Geological Survey, Menlo Park, CA, USA*
[g] *Dipartimento di Scienze Ambientali, Università Ca' Foscari di Venezia Dorsoduro, Venezia, Italy*

Received 14 August 2007; received in revised form 18 December 2007; accepted 15 January 2008

KEYWORDS
Isotopes;
Chemistry;
Tracers;
Water resources;
Salinity;
Morocco

Summary Groundwater and surface water in Souss–Massa basin in the west-southern part of Morocco is characterized by a large variation in salinity, up to levels of 37 g L^{-1}. The high salinity coupled with groundwater level decline pose serious problems for current irrigation and domestic water supplies as well as future exploitation. A combined hydrogeologic and isotopic investigation using several chemical and isotopic tracers such as Br/Cl, $\delta^{18}O$, $\delta^{2}H$, ^{3}H, $^{87}Sr/^{86}Sr$, $\delta^{11}B$, and ^{14}C was carried out in order to determine the sources of water recharge to the aquifer, the origin of salinity, and the residence time of water. Stable isotope, ^{3}H and ^{14}C data indicate that the high Atlas mountains in the northern margin of the Souss–Massa basin with high rainfall and low $\delta^{18}O$ and $\delta^{2}H$ values (−6 to −8‰ and −36 to −50‰) is currently constitute the major source of recharge to the

* Corresponding author. Tel.: +212 28 22 09 57; fax: +212 48 22 01 00.
E-mail addresses: lbouchaou@yahoo.fr (L. Bouchaou), jean-luc.michelot@u-psud.fr (J.L. Michelot), vengosh@duke.edu (A. Vengosh), yhsissou@yahoo.fr (Y. Hsissou), qurtobi@yahoo.fr (M. Qurtobi), cheikh.gaye@gmail.com (C.B. Gaye), tdbullen@usgs.gov (T.D. Bullen), zuppi@tin.it (G.M. Zuppi).
[1] Previous address: Section of Isotope Hydrology, IAEA, Vienna.

0022-1694/$ - see front matter
doi:10.1016/j.jhydrol.2008.01.022

Souss–Massa shallow aquifer, particularly along the eastern part of the basin. Localized stable isotope enrichments offset meteoric isotopic signature and are associated with high nitrate concentrations, which infer water recycling via water agricultural return flows. The ^{3}H and ^{14}C data suggest that the residence time of water in the western part of the basin is in the order of several thousands of years; hence old water is mined, particularly in the coastal areas. The multiple isotope analyses and chemical tracing of groundwater from the basin reveal that seawater intrusion is just one of multiple salinity sources that affect the quality of groundwater in the Souss–Massa aquifer. We differentiate between modern seawater intrusion, salinization by remnants of seawater entrapped in the middle Souss plains, recharge of nitrate-rich agricultural return flow, and dissolution of evaporate rocks (gypsum and halite minerals) along the outcrops of the high Atlas mountains. The data generated in this study provide the framework for a comprehensive management plan in which water exploitation should shift toward the eastern part of the basin where current recharge occurs with young and high quality groundwater. In contrast, we argued that the heavily exploited aquifer along the coastal areas is more vulnerable given the relatively longer residence time of the water and salinization processes in this part of the aquifer.

Introduction

The salinity of water resources has been studied intensively during the past decades, particularly in coastal aquifers, stimulated by both scientific interest and social relevance (Custodio, 1987; Richter and Kreitler, 1993; Appelo and Postma, 1993; Vengosh and Rosenthal, 1994; Calvache and Pulido-Bosh, 1997; Fedrigoni et al., 2001; Al-Weshah, 2002; Vengosh, 2003; Vengosh et al., 2002, 2005, 2007; Petalas and Diamantis, 1999; Farber et al., 2004). Sustainable management of available groundwater reserves is almost impossible without adequate knowledge of the spatial distribution of fresh and saline groundwater and the processes that determine the salinity variations in time and space. As the present-day distribution of fresh and saline groundwater in aquifers still reflects former hydrological conditions, it is often unclear to what extent the current situation is the result of long-term (geological) processes or recent (anthropogenic) changes (Edmunds et al., 2003; Risacher et al., 2003; Vengosh et al., 2005; Boughriba et al., in press; Bennetts et al., 2006). Understanding the processes and factors that control the evolution of saline water in the aquifers over the years is an academic challenge and at the same time has important practical implications for water resource evaluation and management.

In Souss–Massa basin (Fig. 1), situated in the west-southern part of Morocco, agriculture, tourism and sea fishing are the primary economic activities. These various activities require availability of significant water resources. Over the last decades, the region has become one of the major economic growth areas in Morocco. The Souss–Massa hydrological basin covers approximately 27,000 km^2 in which 1500 km^2 lies over the plain. With a year-round growing season, irrigated agriculture in the alluvial basin produces more than half of Morocco's exported citrus and vegetables. The area is characterized by a semi-arid climate and by marked seasonal contrasting climate variables. The rainfall average amounts to 250 mm/year in the plain area and 500 mm/year in the mountain. The annual average temperature ranges between 14 °C and 20 °C in the high Atlas and in the anti-Atlas, respectively, with significantly higher temperature range of up to 48°C in the plain. The range of daily and seasonal temperatures in the plain is also high (19 °C in winter and 27 °C in summer). The precipitation period in a typical year is between October and March and the dry period can extend from April to September. The potential evaporation is very high (>2000 mm/year) in the plain. The rainfall exceeds the evaporation during winter especially in the mountains areas, which constitute the main recharge origin for the Souss–Massa aquifer system.

The rivers of the region, locally called ''oued'', have an intermittent flow regime, because the dry season is typically very long (6–8 months) every year. The main oueds in this basin are the Souss and Massa rivers, which receive many important flow tributaries, in particular from the high Atlas mountains in the north and the anti-Atlas mountains in the south (Fig. 2A).

The plain hosts a large number (more than 20,000) of wells with depths varying from a few meters to nearly 300 m. Most of these wells, which tap a multilayered unconfined aquifer, are penetrated into Plio-Quaternary sands and gravels and supply water for irrigation. Some of the wells are used for drinking water, and only few for industry, and approximately 94% of the water is used for irrigation. These exploitation rates, which are required to meet the increasing demands of the current agricultural practices, exceed the natural replenishment of these basins and had led to depletion of the groundwater resources and degradation of their quality. The total water extraction in the basin is estimated by the local water authorities as 650 million cubic meters per year. On average, groundwater extraction in the basin exceeds recharge by an estimated 260 million cubic meters annually (D.R.P.E., 2004). This over-pumping of the alluvial aquifer has resulted in water level declines ranging from 0.5 to 2.5 m/year during the past three decades. The water quality is highly variable and in some areas reaches high salinity levels exceeding 37 g L^{-1} (Hsissou et al., 1999). Evaluation of the mechanisms that cause the degradation of the groundwater quality in the Souss–Massa basin is the focus of this paper.

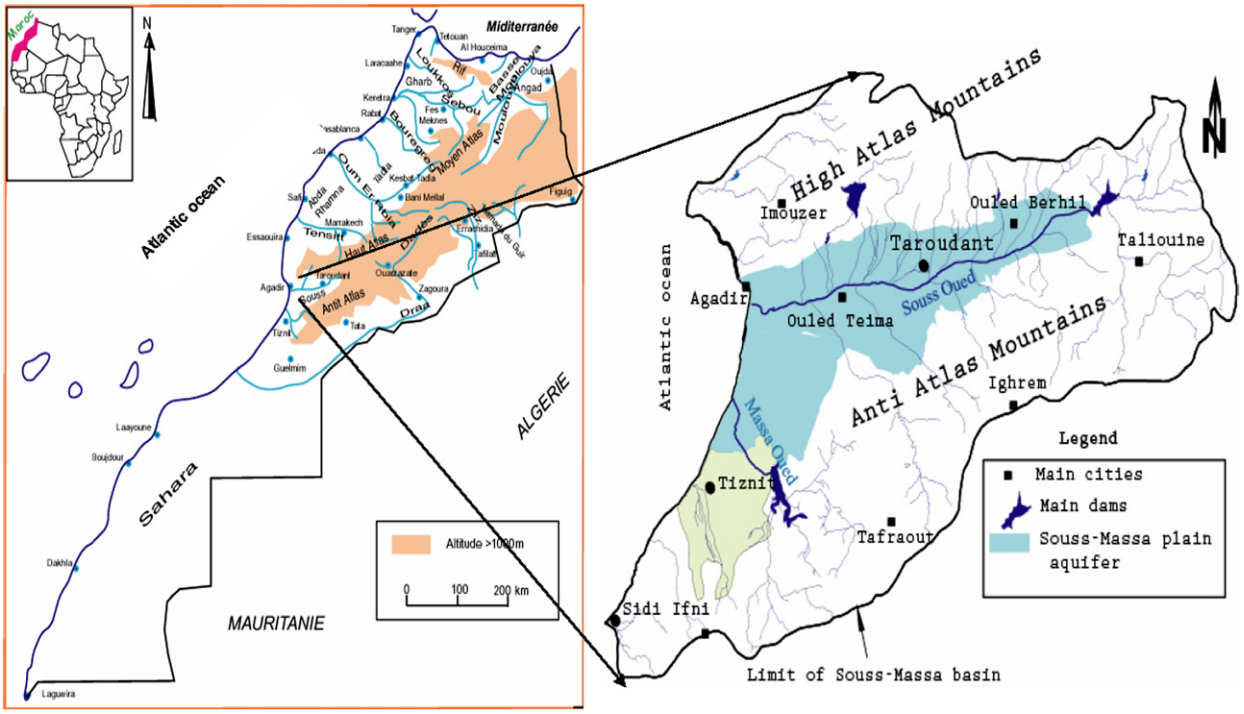

Figure 1 General and detailed maps of the Souss—Massa basin in the west-southern part of Morocco.

Previous chemical and stable isotopic (for only $\delta^{18}O$ and $\delta^{2}H$) data (Boutaleb et al., 2000; Hsissou et al., 2001; Ekwurzel et al., 2001; Hsissou et al., 2002; Ahkouk et al., 2003; Dindane et al., 2003; Krimissa et al., 1999; Bouchaou et al., 2003, 2005) provided preliminary indications on chemical and isotopic water characterization. These studies have suggested that the principle sources that effect groundwater quality are: (1) water—rock interactions and dissolution of evaporitic rocks from marginal areas, (2) modern seawater intrusion, and (3) anthropogenic pollution. The aim of this paper is to further evaluate the processes that affect the groundwater quality in the Souss—Massa basin by using a larger set of isotopic and geochemical tools. We employ a multiple isotope approach ($\delta^{18}O$, $\delta^{2}H$, ^{3}H, $^{87}Sr/^{86}Sr$, $\delta^{11}B$, $\delta^{13}C$ and ^{14C}C) for delineating water and salt sources and modeling mixing phenomena in the aquifer. The overall objective of this study is to provide reliable tools for understanding groundwater quality degradation under conditions of over-exploitation in semi-arid zones. We posit that integration of hydrological, geochemical, and multiple isotopic tracers provide crucial information for successful management of the water resources under instable hydrological conditions where exploitation exceeds replenishment.

Geology and hydrogeology settings

The Souss—Massa plain is an alluvial depression between the high Atlas in the north and the anti-Atlas mountains in the south. The age of the geological formations ranges from Paleozoic to Quaternary. The plain is composed of Plio-Quaternary sediments (sands, gravels and lacustrine limestone), which covers a Cretaceous syncline in the north of the basin, and a Palaeozoic schistose basement in the south (Fig. 2A). The Plio-Quaternary strata in the plain are locally heterogeneous both in vertical and lateral directions. The thickness of the aquifer increases from east (30 m) to west (>200 m). The syncline axis is oriented on east—west direction (Fig. 2B). Its northern flank outcrops vertically in the high Atlas and marks a vertical fault, which is known as the South-Atlas fault. Its southern short flank outcrops slightly in the centre of the basin. The high Atlas shows an alternation of permeable and impermeable Mesozoic formations. Some layers contain evaporates minerals (gypsum in Jurassic and Cretaceous, and halite in Triassic formations). The Cretaceous layers resulting from the major transgression in the area, underlain the plain (Fig. 2B). This is confirmed by data revealed from boreholes that penetrated rocks from surface alluvium through Turonian-age rocks. The deep boreholes and geophysical measurements have shown a large variability in the substratum (Ambroggi, 1963; C.A.G., 1963).

The anti-Atlas Mountains are characterized by carbonate and crystalline formations. The presence of evaporite layers in the Mesozoic formations of the southern side of the high Atlas is likely to influence the water quality of the oueds (temporary rivers) that drain this side of the aquifers and those of the piedmonts. Succession of the Atlantic transgressions between Cretaceous and Quaternary can explain the variation of marine facies in the basin. The major marine incursion was arrived during the Cretaceous period and the latest humid period was in the Holocene (Weisrock, 1980; Weisrock et al., 1985). The Holocene African humid period occured between 9 and 6 ky BP. The level of marine incursion were about 2 m above the present one.

The faulted structure of the Cretaceous—Eocene syncline can also allow hydrodynamic relations between the

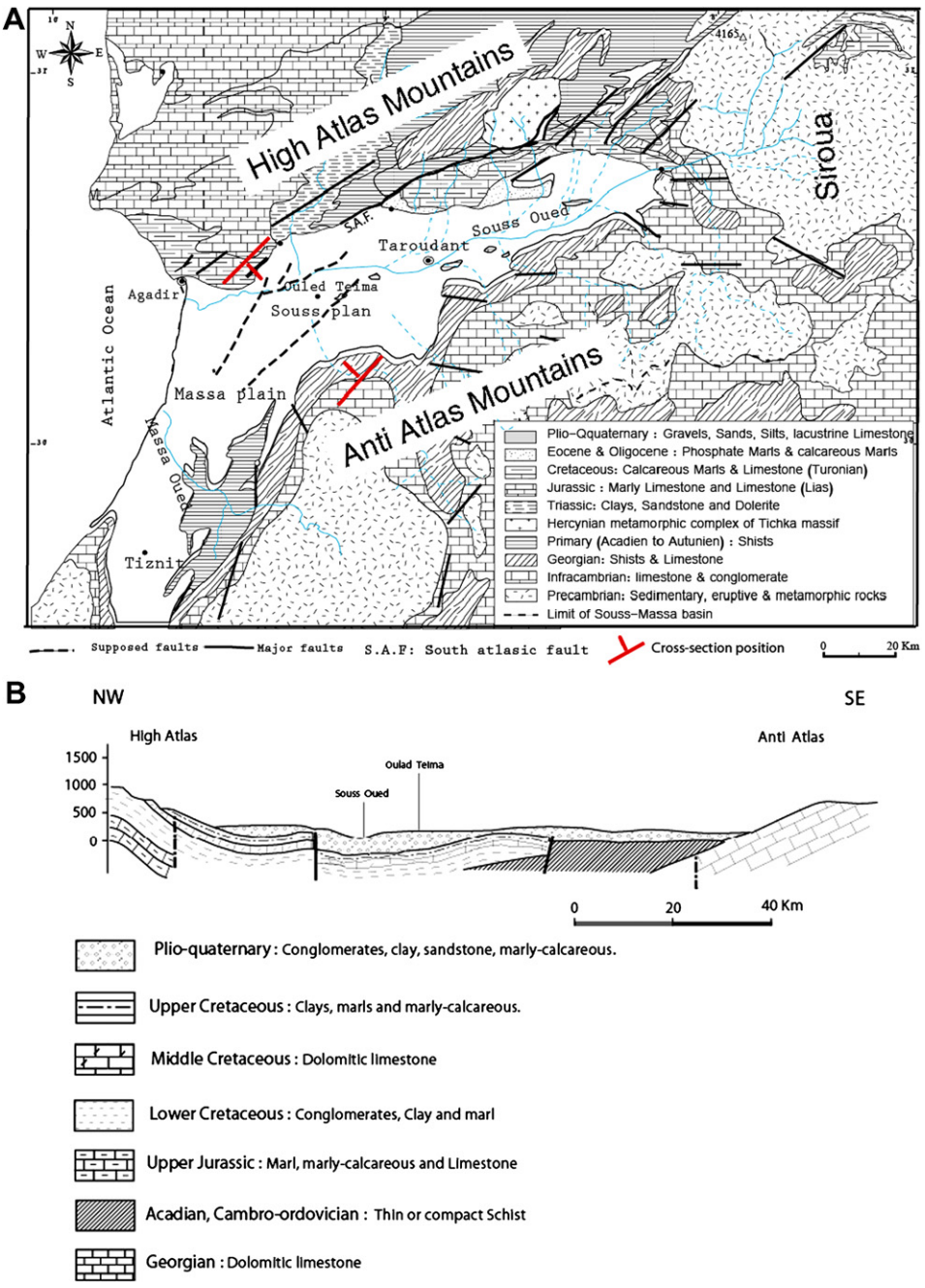

Figure 2 (A) Geological map of the Souss—Massa basin; (B) A geological cross-section in the studied area (position marked in (A).

different aquifers of the plain. The principal water resource is provided by the Souss—Massa Plio-Quaternary plain aquifer and by the dams (Fig. 1). The sand and gravel aquifer, which was previously mainly exploited for irrigation, is becoming a source of increasing importance for the domestic supply of the Souss—Massa region. Groundwater occurs under unconfined conditions in the Pliocene and Quaternary formations of the plain, often overlying one or several confined sub-aquifers, like the Turonian aquifer (Dijon, 1969; Combe and El Hebil, 1977). The unconfined groundwater is the main water resource of this multi-strata system, which shows a high variability of the transmissivity values (10^{-4} to 10^{-1} m^2/s). The maximum values are found around the Souss oued like sediments (conglomerates, sands and lacustrine limestone) corresponding to the old bed oueds that creates preferential flow paths of the groundwater. The geology of many wells reflects the lateral and vertical heterogeneity of this shallow aquifer. The soils of Souss—Massa plain are diversified; ranging from sandy-loam soils with low humus content and relatively high permeability to soils with high clay contents. The former soil types are characterized by a coarse texture with low content of clay minerals and occur mainly in the Chtouka—Massa region and in Atlas foothills surrounding the Souss plain. The later soil types are xeric, brown-to-black, and having clayey—sand texture with moderate amounts of clay minerals.

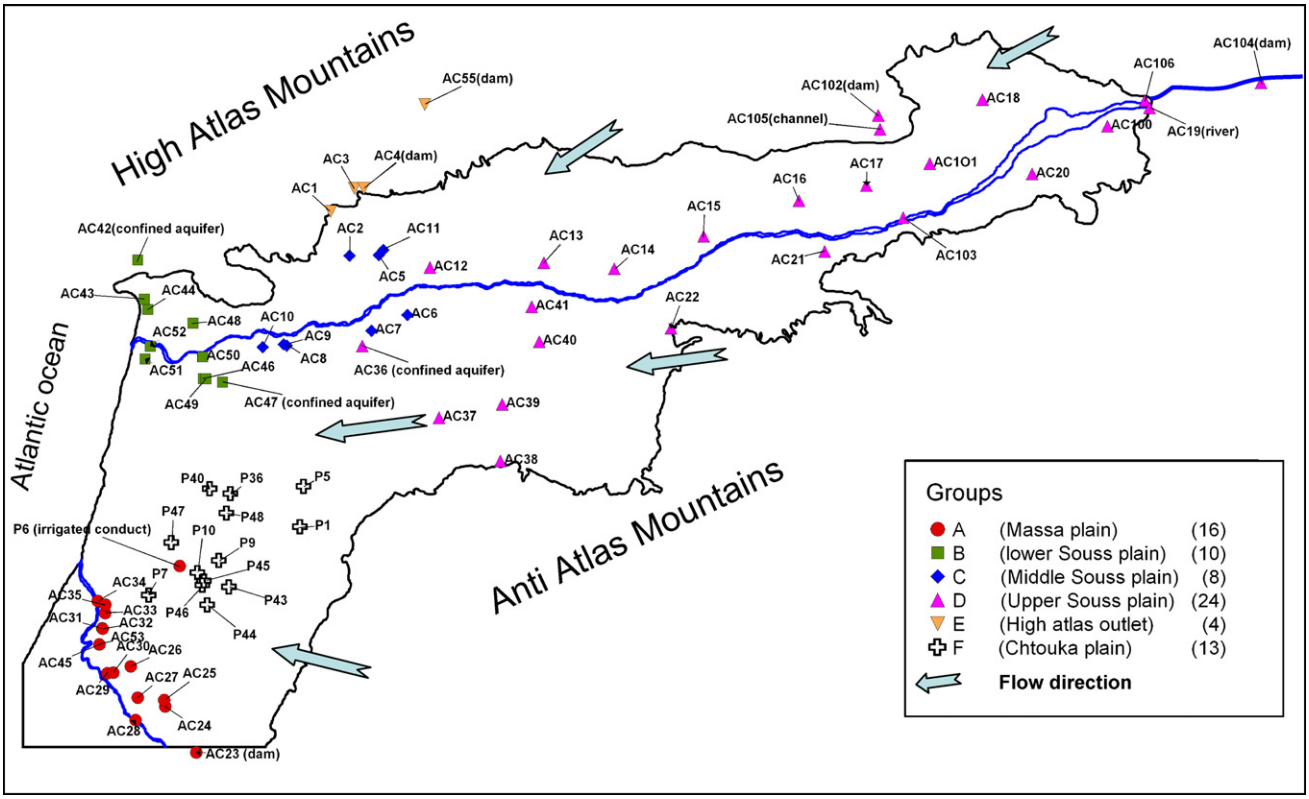

Figure 3 Sampling points of wells and surface water in Souss–Massa basin, sorted by their geographical distribution (defined as water groups, see Table 1). The general groundwater flow directions in the basin are also included.

The piezometric survey shows a flow direction from east to west towards the Atlantic ocean, which constitutes the main outlet of Souss–Massa aquifer (Fig. 3). The major drainage axis appears along the Souss Oued. The riverbeds have good permeability and constitute an appropriate site for numerous pumping wells. This structure represents the area where the risk of salinization of the groundwater by seawater intrusion is high, in particular in the coastal areas.

Method and sampling analyses

About 80 water samples were collected during two sampling campaigns over a two-year period (2000–2001) from surface water bodies (dams and oueds), wells, boreholes and springs in various parts of the basin (Fig. 3), and were analyzed for their chemical and isotopic compositions. Temperature, pH, Electrical conductivity (EC) and total alkalinity were measured in the field. Water samples were collected from pumping wells after minimum of several hours of pumping prior to sampling. Chemical analyses of major elements were carried out in several laboratories, including the ''Applied Geology and Geo-Environment Laboratory'' of the University of Agadir in Morocco, the ''Analytical Laboratory'' of the Department of Geological and Environmental Sciences, Ben Gurion University of the Negev in Israel, and the IAEA laboratories in Vienna. Analytical error as inferred from the balance between cations and anions did not exceed 5%. Trace elements (B, Sr) were measured at the analytical laboratory of the Department of Geological and Environmental Sciences, Ben Gurion University of the Negev and at the Department of Geology and Geochemistry, Stockholm University in Sweden. Cations and boron were determined by ICP and anions by IC. The ^{14}C activity (pmc) and ^{13}C vs. ‰ vs. PDB (Craig, 1957) were measured at the IDES Laboratory ''ex Laboratoire d'Hydrologie et de Géochimie Isotopique'' of Orsay, Paris, France, with a precision of 0.4 pmc and 0.15 % for ^{14}C and $\delta^{13}C$, respectively. Stable isotopes of oxygen and hydrogen as well as tritium were analyzed at the Isotope Laboratory of the ''Centre National des Sciences and Technologies Nucléaires (CNESTEN), Rabat, Morocco''. Tritium concentrations are expressed in Tritium Units with a precision of ±0.5. Oxygen ($\delta^{18}O$) and hydrogen ($\delta^{2}H$) isotopes are reported relative to Vienna-standard mean ocean water (VSMOW) and expressed in delta values with a reproducibility of ±0.1‰ and ±1‰, respectively. Boron isotopes were measured by a negative thermal ionization mass spectrometry technique. The NIST SRM-951 standard was used and $^{11}B/^{10}B$ ratios are reported as $\delta^{11}B$ values. Strontium was separated via ion-exchanger using Biorad AG50X8 resin at Ben Gurion University and the isotopic ratios were measured by thermal ionization mass spectrometry (MAT-261) at the US Geological Survey, Menlo Park, California, USA. An external precision of 2×10^{-5} ‰ for the Sr isotope measurements was determined by replicate analyses of the NIST-987 standard. Laboratory preparation and mass spectrometry procedures are identical to those described in Bullen et al. (1996).

Results and discussion

Tables 1 and 2 present the chemical and isotopic data for the two sampling campaigns (2000 and 2001), respectively. The data and the following discussion are presented according to the geographical distribution of the wells in the basin (Fig. 3) and the conceptual cross-section of the aquifer (Fig. 2A). The salinity (TDS) of the investigated water range from 350 to 37,000 mg/L. We define water with salinity lower than 1000 mg/L as freshwater.

Tracing groundwater recharge

In spite of the scarcity of rain measurements in the Souss–Massa area, previous observations have shown relatively high $\delta^{18}O$ and $\delta^{2}H$ values in rainwater over the Souss–Massa plain relative to much lower values over the mountains (Bouchaou et al., 2005). Thus rain water measured in the Agadir gauge on the coast has a significantly higher $\delta^{18}O$ value ($-4‰$) relative to the much depleted ^{18}O signature in rain in mountain gauges ($-7.5‰$ at 1000 m a.s.l.) measured in the Issen basin within high Atlas mountains. This distinction enables us to hypothesize two types of recharged waters: (1) local rain with high $\delta^{18}O$ and $\delta^{2}H$ values; and (2) high elevation rain over the high Atlas and anti-Atlas mountains with low $\delta^{18}O$ and $\delta^{2}H$ values. The latter water source is not a direct recharge but rather reflects lateral flow from the mountains areas.

The $\delta^{18}O$ and $\delta^{2}H$ values of fresh water (<1000 mg/L) from the investigated water are plotted and compared with the global meteoric world line (GMWL; Rozanski et al., 1993) with deuterium excess = 10‰ (Fig. 4). The data show that most of the fresh groundwater from the Souss–Massa basin has $\delta^{18}O$ values that are closed to the GMWL. Moreover, the data show that groundwater from the upper and middle Souss Plain has $\delta^{18}O$ values between $-6‰$ and $-7.8‰$ whereas groundwater from the coastal areas from the lower Souss and Massa plains have higher $\delta^{18}O$ values, in the range of $-0.3‰$ to $-6.5‰$ (Fig. 4). This distinction suggests that groundwater recharge in the lower Souss and Massa plains (Fig. 3) can occur in part from local and coastal rains with higher $\delta^{18}O$ values combined with recharge of the upper Souss groundwater, while water sources in the middle and upper Souss basins are derived mainly from lateral flow of groundwater, originally recharged over high elevation in the mountains with low $\delta^{18}O$ values. Bouchaou et al. (1995) have shown isotope gradient of 0.26‰ of $\delta^{18}O$ values per meter altitude. The $\delta^{18}O$ variations (-5.6 to $-7.5‰$; Tables 1 and 2) in the fresh groundwater (TDS < 1000 mg/L) of the upper and middle Souss basins suggest that groundwater recharge in the study area originates from both high altitudes (600–1900 m) rain with a mean $\delta^{18}O$ signature of $-7‰$ and local meteoric water with a lower $\delta^{18}O$ value. It seems that mountain recharge is not available for the coastal groundwater and thus the water resources in these regions are more limited for predominately local recharge. In the same time, the source of groundwater in the upper and middle Souss plain is derived from external sources; lateral groundwater flow originated in the high Atlas and anti-Atlas mountains. This contribution is favored by the high permeability and soil structure in this area.

In addition to the local recharge water, mixing with external saline sources as well as surface evaporation could potentially modify the stable isotope composition of the investigated water. In both scenarios, the $\delta^{18}O$ and $\delta^{2}H$ values would deviate from the GMWL slope towards elevated $\delta^{18}O$ and $\delta^{2}H$ values with a lower $\delta^{18}O/\delta^{2}H$ slope (Fig. 4). Our data show that some groundwater samples have elevated chloride (>100 mg/l) and nitrate (>50 mg/l) concentrations that are associated also with relatively high $\delta^{18}O$ values (Fig. 5A and B). In the coastal areas (Massa and Chtouka plains) recharge of nitrate-rich water increases the $\delta^{18}O$ to $-4‰$ while in the middle Souss plain, the $\delta^{18}O$ is modified from $\sim-7.5‰$ to $-6‰$ (Fig. 5A). This association might suggest that recycling of agricultural return flows (Ahkouk et al., 2003) is an important recharge source in the coastal area. This source is distinguished by high nitrate, $\delta^{18}O$, and $\delta^{2}H$ values. Consequently, we suggest that overexploitation of local groundwater combined with massive agricultural utilization, particularly in the Massa, middle Souss, and Chtouka plains, have resulted in formation of agricultural return flows that have penetrated into the pumping zones in the aquifer. This recharge component represents anthropogenic activities and causes direct degradation of the water quality of the aquifer due to the high nitrate that is associated with this source. From a water management prospective, future exploitation of the aquifer in these areas will become limited for only agricultural utilization given the high nitrate levels that are expected to increase with higher contribution of this water source. Moreover, any attempts to evaluate hydrological balances and safe yields of groundwater resources in these areas must take into consideration the fact that an important component of the recharge is derived from recycling of groundwater and not from external natural replenishment.

The origin of water salinity

Chemical characteristics

The salinity of the groundwater is determined by the total dissolved solids (TDS). The chemical variations (Table 1) show three types of saline water with different proportions of the major dissolved constituents (Fig. 6): (1) water with high Cl/TDS and relatively low SO_4/TDS ratios in which Na and Cl ions consist of the major dissolved salts (Fig. 6A); (2) water with low Cl/TDS and relatively high SO_4/TDS ratios in which sulfate content controls the TDS (Fig. 6B); and (3) water with relatively high NO_3/TDS ratios (Fig. 6C). Saline waters of Type 1 are identified in groundwater samples from the coastal areas (Massa, Low Souss, and Chtouka plains; Fig. 3) as well as in the middle Souss plain and high Atlas outlet. Saline waters of Type 2 are identified also at middle Souss plain and high Atlas outlet. High nitrate groundwater (>50 mg/L) occurs in the Massa, Chtoouka and middle Souss plains.

High Cl/TDS type water. Along the coastal areas (Massa, low Souss, and Chtouka plains) the groundwater with the high Cl/TDS ratios are characterized by low Na/Cl (<1), SO_4/Cl, and Ca/Cl ratios and marine ($\sim1.5\times10^{-3}$) Br/Cl ratios. These geochemical variations characterize seawater intrusion (Vengosh, 2003) and thus suggest that seawater intrusion is the predominant source for groundwater salini-

Table 1 Chemical and isotope (stable isotopes of oxygen and hydrogen and tritium) data in Souss–Massa basin (results from 2000 and 2001 sampling campaigns)

Code	Nature	Name	Year	T °C	E.C. (µs cm^{-1})	pH	Ca	Mg	Na	K	Cl	HCO_3	SO_4	NO_3	Br	TDS	Na/Cl (molar)	SO_4/Cl (molar)	Br/Cl (molar)	$\delta^{18}O$ (‰)	$\delta^{2}H$ (‰)	^{3}H (TU)
Massa plain (Group A)																						
AC23	Dam	Retennu du B,Y,T	2000	20	515	8.1	21.6	23	45	2.7	71	174	15	3.6	0.274	356	0.98	0.078	1.71E−03	−0.3	−4.9	2.7
P6	Channel	Canal d'irrigation	2000	19	583	8	42	11	31.1	1.9	62	149	20	5	nd		0.77	0.119		−2.19	−13.6	nd
AC24	Well	Puits de Qsebt	2000	23	13610	8	276	265	2250	19.4	3976	1224	225	0.8	12.21	8248	0.87	0.021	1.36E−03	−1.2	−4.8	1.7
AC25	Well	Puits à cöté de AC24	2000	25	4970	7.2	107.2	149	740	4.8	1136	519	270	27	3.536	2957	1.00	0.088	1.38E−03	−3.4	−23.7	0.3
AC26	Well	Puits El Mers	2000	24	7340	6.9	186.4	369	710	10.2	2237	276	80	85.6	7.046	3961	0.49	0.013	1.40E−03	−3.3	−20.4	0.3
AC27	Well	Puits Ait Oumribt	2000	24	5440	7.7	62.4	96	810	8	1356	389	108	91.8	4.443	2926	0.92	0.029	1.45E−03	−3.5	−22.8	1.3
AC28	Well	Puits Tibouzar	2000	23	3650	7.5	46.4	101	540	1.6	888	321	66	57.5	2.876	2024	0.94	0.027	1.44E−03	−4.5	−27.9	0.4
AC29	Well	Puits Mr Slimane	2000	14	1182	8	36	49	104	6.9	178	272	62	0.1	0.673	709	0.90	0.129	1.68E−03	−1.5	−11.2	2.8
AC30	Well	Puits à cöté de AC29	2000	14	1100	8.2	40	44	95	6.7	178	247	56	4.7	0.609	672	0.82	0.116	1.52E−03	−1.8	−11.4	
AC31	Spring	Source de Talat N'oungalf	2000	23	1157	7.7	40	75	74	2.6	142	377	46	24.5	0.638	782	0.80	0.120	1.99E−03	−6.1	−37.4	0
AC32	Well	Puits à cöté de AC31	2000	23	1288	7.6	44	81	86	3.4	192	379	68	20.5	0.412	874	0.69	0.131	9.52E−04	−6.2	−38.8	
AC33	Spring	Source Aghbalou	2000	25	1193	8	44	81	75	3	178	333	66	15.8	0.62	796	0.65	0.137	1.55E−03	−6.3	−40.8	0
AC34	River	Pont sur oued Massa (aval Aghbalou)	2000	19	11220	7.9	90.4	374	1580	1.2	3181	482	320	2.7	11.55	6043	0.77	0.037	1.61E−03	−2.9	−15.3	
AC35	Well	Puits de Mr KILANI	2000	24	2120	7.5	45.6	102	153	5	462	277	90	17.1	1.346	1153	0.51	0.072	1.29E−03	−6.1	−40.7	0
AC53	Borehole	ONEP collège El Massira (Massa) no. 2	2000				51.2	106	218	3.4	525	336	96	46.4	1.691	1384	0.64	0.068	1.43E−03	−4.9	−31.2	0
AC24	Well	Puits de Qsebt	2001	24.6	4267	6.8	139.7	80.2	693.8	5.38	991.0	401.8	265.8	139.2	3.35	2720	1.08	0.099	1.50E−03	−3.71	−20.3	1.7
AC60	Well	Source Agbalou	2001	25	987	7	69.8	57.7	80.3	2.77	197.6	280.8	44.4	25.1	0.78	759	0.63	0.083	1.75E−03	−6.45	−37.35	0
AC61	Well	Forrage ONEP Massa	2001	23.7	818	6.9	77.3	49.8	59.4	1.92	117.6	353.9	36.9	27.7	0.44	725	0.78	0.116	1.66E−03	−6.05	−43.15	
AC33	River	Station Belfaa	2001	25.1	1164	7.7	100.4	65.3	105.3	2.25	245.8	387.0	46.3	42.2	0.78	995	0.66	0.070	1.41E−03	−5.4	−38.85	
Lower Souss plain (Group B)																						
AC42	Borehole	F,A	2000	43	3260	7.5	493.6	180	140	2.1	99	244	1 600	2.2	0.219		2.18		9.82E−04	−5.3	−25.4	0
AC43	Borehole	Jardin Ibn Zaidoun	2000	23	7140	6.9	56	259	1 200	7.9	1864	588	350	11.5	6.677			0.069	1.59E−03	−4.8	−28.7	nd

(*continued on next page*)

Table 1 (*continued*)

Code	Nature	Name	Year	T °C	E.C. (µs cm^{-1})	pH	Ca	Mg	Na	K	Cl	HCO_3	SO_4	NO_3	Br	TDS	Na/Cl (molar)	SO_4/Cl (molar)	Br/Cl (molar)	$\delta^{18}O$ (‰)	$\delta^{2}H$ (‰)	^{3}H (TU)
AC44	Borehole	Puits no. 51	2000	24	7360	6.8	340.8	264	600	9.9	2077	386	320	20.8	6.264	4025	0.45	0.057	1.34E−03	−5.9	−37.3	0.3
AC45	Borehole	Forage ONEP	2000	25	2260	7.4	72	81	280	3.2	462	361	108	40.2	1.55	1409	0.93	0.086	1.49E−03	−4.8	−30.2	0
AC46	Borehole	No. 8 Petromin Al Hana (Ait Melloul)	2000	25	3930	7.1	54.4	221	360	6	710	520	300	4.5	2.695	2179	0.78	0.156	1.68E−03	−6.9	−44.2	0.4
AC47	Borehole	Forage Ferrugineux Kléa	2000	30	1976	7	103.2	122	136	13	238	437	375	0.3	0.566	1425	0.88	0.582	1.06E−03	−4.9	−34.3	0
AC48	Borehole	Puits ONEP club Med	2000	23	2440	7	100	138	255	3.8	440	395	325	4.9	0.927	1663	0.89	0.273	9.35E−04	−6.1	−38.7	1.4
AC49	Borehole	Petrromin oil Al farah (Ait Melloul)	2000	26	1514	7.4	88.8	75	114	3.2	234	376	124	5.1	0.709	1021	0.75	0.196	1.34E−03	−7.4	−47.5	0.2
AC50	Borehole	ONEP Ait Melloul	2000	25	1755	7	68	132	98	3	238	510	116	14.9	1.093	1181	0.63	0.180	2.04E−03	−7	−44.5	0
AC51	Borehole	Forage Reserve Royal	2000	23	621	7.8	31.2	22	78	6.4	82	232	22	18	0.185	492	1.47	0.099	1.00E−03	−4.1	−22.7	0
AC52	Well	Royal sur la berge de l'oued	2000	20	2550	8	37.6	38	410	43	522	554	28	2.6	nd	1635	1.21	0.020	nd	nd	nd	nd
AC43	Well	Jardin bnou Zaidoun	2001	24	4118	6.6	195.5	217.2	1066.3	8.03	2079.0	377.5	569.8	33.2	6.18	4553	0.79	0.101	1.32E−03	−4.71	−24.6	nd
AC44	Well	Puits no. 51	2001	29.1	8426	6.7	413.8	396.7	942.5	12.43	2747.0	255.7	551.2	26.5	8.49	5354	0.53	0.074	1.37E−03	−5.84	−29	0.3
AC46	Well	No. 8 Petromen Al Hana	2001	24.9	1031	7.3	73.8	51.7	77.4	3.05	98.9	357.8	103.7	14.1	0.29	781	1.21	0.387	1.30E−03	−7.81	−47.75	0.4
AC47	Well	Forrage ferrugeneux Klea	2001	31	2039	6.8	113.3	79.4	147.1	38.08	186.8	254.4	474.1	2.9	0.70	1297	1.21	0.937	1.66E−03	nd	nd	0
AC49	Well	Petromin oil Al farah (Ait Melloul)	2001	25.6	1645	7.2	96.7	84.8	113.0	3.04	278.3	325.9	150.6	17.5	1.02	1071	0.63	0.200	1.63E−03	−7.19	−47.9	0.2
AC50	Well	ONEP Ait Melloul	2001	24.8	1666	6.5	87.9	102.4	83.0	6.30	235.3	404.4	113	66.2	0.74	1099	0.54	0.177	1.39E−03	−6.82	−45.45	0
AC58	Well	ONEP Lmzar forrage, °10	2001	24.4	1549	6.9	88.4	86.3	191.0	3.30	377.4	357.3	126.6	32.7	1.41	1264	0.78	0.124	1.66E−03	−6.56	−46.3	nd
AC59	Well	ONEP Lmzar forrage, °8	2001	24.9	1388	7	55.8	55.1	154.8	2.91	207.6	342.5	93.5	21.9	0.74	935	1.15	0.166	1.59E−03	−6.4	−45.75	nd
Middle Souss plain (Group C)																						
AC6	Well	118 briquettrie	2000	23	2050	7.2	108.8	126	120	6.6	320	336	150	53.1	0.98	1221	0.58	0.173	1.35E−03	−6.5	−41.2	0.6
AC7	Well	Puits pour l'AEP(120)	2000	23	2480	7	132	163	144	2.4	405	443	290	27	1.85	1608	0.55	0.264	2.03E−03	−5.7	−37.2	1.8
AC8	Well	Douar Bouzoug	2000	25	1062	7.1	90.4	42	44	2	111	225	100	10	0.20	625	0.61	0.333	8.15E−04	−7.4	−47.9	0
AC9	Well	Puits ferme de AAMI	2000	23	2220	7.1	133.6	118	96	2.2	398	487	110	5.6	1.48	1352	0.37	0.102	1.65E−03	−6.3	−38.6	nd
AC10	Well	Briquetterie à cöté DE la station schell Temsia	2000	24	1092	7.2	72	84	30	2.2	131	438	40	2	0.49	800	0.35	0.113	1.66E−03	−7	−42.8	0
AC11	Well	Puits à cöté du no. 60	2000	22	3320	7.4	126.4	35	500	5.4	742	390	98	3.5	0.21	1901	1.04	0.049	1.27E−04	−5.6	−37.8	2.6
AC6	Well	Briquetterie	2001	22.7	1886	7.4	67.9	134.6	127.6	5.96	318.7	306.9	183.4	103.5	1.13	1250	0.62	0.213	1.57E−03	−6.27	−37.95	0.6
AC7	Well	Puits pour l'AEP	2001	22.4	1947	7.4	92.1	96.2	122.4	1.94	367.0	341.5	34.1	46.1	1.54	1103	0.51	0.034	1.87E−03	−6.56	−38.9	1.8

AC8	Well	Douar Bouzoug	2001	24.1	947	7	65.8	59.9	40.9	2.12	77.0	365.7	70.7	8.7	0.29	691	0.82	0.339	1.70E−03	−7.63	−46.85	0
AC9	Well	Puits ferme de AAMI	2001	21.7	1958	6.8	129.2	149.6	112.9	2.36	458.0	370.2	105.2	147.9	2.04	1477	0.38	0.085	1.98E−03	−6.18	−38.65	nd
Upper Souss plain (Group D)																						
AC12	Well	Ferme de Mr Houjhaij aissa	2000	25	800	7.1	92.8	20	45	1.4	71	336	14	14.2	0.20	595	0.98	0.073	1.27E−03	−5.8	−33.2	0
AC13	Well	Puits au Nord du no. 68 (Baäkla)	2000	25	1187	7.1	143.2	47	49	1.3	67	303	265	12.8	0.11	888	1.13	1.461	7.42E−04	−7	−46.2	0
AC14	Well	Puits no. 76	2000	23	975	7.2	104	39	49	1.6	64	368	64	2.7	0.13	692	1.18	0.369	9.15E−04	−7.4	−47.4	1.3
AC15	Well	Puits Ait Iazza	2000	23	990	7.2	102.4	27	65	1.2	53	387	70	6.8	0.12	713	1.89	0.488	1.03E−03	−7.5	−50.3	0
AC16	Well	Puits de l'ORMVA	2000	24	953	7.3	97.6	42	30	2.2	57	306	84	12.2	0.12	631	0.81	0.544	9.42E−04	−7.2	−46.8	1.3
AC17	Borehole	Ferme de Mr KAYOUH Hassan	2000	22	867	7.3	107.2	25	27	1.9	43	306	68	2.5	0.12	581	0.97	0.584	1.27E−03	−7.5	−48.1	1.9
AC18	Borehole	Ferme de Mr ELOUAFI	2000	25	1260	7.3	155.2	50	28	2.2	28	277	330	5	0.07	875	1.54	4.352	1.13E−03	−6.9	−44.9	0
AC19	River	Pont Aoulouz	2000	17	445	8.7	40	19	23	3.6	21	206	26	1.9	0.06	341	1.69	0.457	1.25E−03	−7.2	−47.3	5.5
AC20	Well	Puits Mr Haj Omar Ait Si	2000	22	611	7.6	51.2	25	28	2.3	28	293	38	6.6	0.07	472	1.54	0.501	1.17E−03	−6.8	−43.5	0
AC21	Well	Puits station Agip à Arazane	2000	23	916	7.2	69.6	57	36	3.3	53	414	46	2.2	0.21	681	1.05	0.320	1.73E−03	−6.7	−43.9	0.9
AC22	Well	Puits au dessous de Ras El Ain	2000	25	920	7.2	73.6	57	36	2.8	71	367	46	19.4	0.35	673	0.78	0.239	2.21E−03	−6.1	−38.9	0.8
AC36	Borehole	Forage Saouda	2000	27	940	7.1	86.4	48	52	2.6	67	349	128	29.5	0.15	763	1.20	0.705	1.01E−03	−6.9	−45.7	0.8
AC37	Well	Puits no. 87	2000	26	1012	7.2	85.6	64	14	1.6	146	290	28	10	0.55	640	0.15	0.071	1.67E−03	−6.6	−43.6	
AC38	Spring	Source Tidsi	2000	26	678	7.6	57.6	52	12	2	38	342	33	4.6	0.15	541	0.49	0.321	1.75E−03	−7	−43.1	0
AC39	Well	Puits no. 95	2000	27	662	7.3	66.4	39	14	1.6	46	298	36	10.8	0.21	512	0.47	0.289	2.04E−03	−6.6	−36.9	0
AC40	Well	Puits no. 96 de Mr BOUAB	2000	21	964	7.2	83.2	58	42	1.8	67	449	76	2.6	0.21	780	0.97	0.419	1.38E−03	−6.8	−41.9	0.3
AC41	Well	puits no. 113	2000	25	1110	7.1	99.2	62	64	2	78	420	140	22.7	0.23	888	1.27	0.663	1.31E−03	−6.8	−43.9	1.8
AC100	Spring	S. Aït Abdelah	2000	20	739	7.6	64	39	27	2.3	28	379	44	8.5	nd	592	1.49	0.580		−6.36	−38.5	nd
AC1O1	Spring	S. Aïn El Jadida	2000	24	1277	7.5	124	38	33	2.5	43	370	145	11.4	nd	767	1.18	1.245		−6.93	−43.6	nd
AC102	Dam	Retenue Bg. Imi El khneg	2000	21	419	8.2	40.8	17	22	4.1	28	145	66	0.5	nd	323	1.21	0.870		−5.11	−34.6	nd
AC103	Channel	Canal d'irrigation Izaid	2000	22	554	8	54.4	25	25	1.9	28	282	40	7.2	nd	464	1.38	0.528		−6.88	−43.8	nd
AC104	Dam	Barrage Chakoukane	2000	21	950	8.1	75.2	49	55	4	50	531	12	2	nd	778	1.70	0.089		−5.85	−39.1	nd
AC105	Dam	Aval du barrage Imi El khenge	2000	24	625	8.3	51.2	25	34	6.5	50	204	76	0.9	nd	448	1.05	0.561		−1.09	−16.1	nd
AC106	Spring	S. Tamgoute	2000	19	505	7.8	41.6	25	19	2.1	21	231	26	3.8	nd	370	1.40	0.457		nd	nd	nd
AC14	Well	Puits Ait Iazza	2001	22.7	975	7.2	104	39	49	1.6	64	368	64	3	nd	693	1.18	0.369		−7.35	−48.3	1.3
AC16	Well	Puits de l'ORMVA	2001	23.8	830	7.63	82	34	33	2.3	36	216	130	1	nd	534	1.41	1.333		−7.79	−46.45	1.3
AC18	Borehole	Ferme de Mr ELOUAFI	2001	22.6	760	7.6	74	38	18	1.9	28	377	22	5	nd	564	0.99	0.290		−7.26	−42.45	0
AC21	Well	Puits station Agip à Arazane	2001	23.5	957	7.13	84	48	35	2.9	43	414	70	18	nd	715	1.26	0.601		−6.9	−43.4	0.9

(*continued on next page*)

Table 1 (*continued*)

Code	Nature	Name	Year	T °C	E.C. (µs cm^{-1})	pH	Ca	Mg	Na	K	Cl	HCO_3	SO_4	NO_3	Br	TDS	Na/Cl (molar)	SO_4/Cl (molar)	Br/Cl (molar)	$\delta^{18}O$ (‰)	$\delta^{2}H$ (‰)	^{3}H (TU)
High Atlas outlet (Group E)																						
AC1	Spring	Source Amskroud	2000	24	2950	6.7	320	293	30	2.9	43	288	1500	6.3	0.09	2483	1.08	12.882	9.29E−04	−6.3	−33.2	3.1
AC2	Well	Puits no. 59	2000	25	1992	6.8	160	163	54	2.9	71	389	650	58.4	0.17	1548	1.17	3.381	1.08E−03	−5.6	−30.9	0
AC3	River	Bou El Baz	2000	13	59000	7.9	585.6	53	14700	19.3	20768	235	1020	5.7	1.66	37388	1.09	0.018	3.55E−05	−4.2	−17.4	1.9
AC5	Well	Puits no. 60	2000	24	2950	7.2	164	37	250	3.9	568	317	132	0.8	0.16	1473	0.68	0.086	1.25E−04	−6.3	−38.4	1.5
AC55	Dam	B. Abdel-Moumen	2000	nd	nd	nd	nd	nd	nd	nd	nd	nd	nd	nd	nd					−5.38	−38.3	nd
AC4	Dam	B Dkhila	2000	21	954	7.8	44.8	46	88	3	128	283	100	0.2	0.15	693	1.06	0.288	5.10E−04	−4.1	−29.5	nd
AC1	Spring	Source Amskroud	2001	24.1	2777	6.5	618.7	122.1	29.3	2.98	38.8	206.2	1769	1.4	0.12	5572.4	1.16	16.839	1.37E−03	−5.93	−32.05	3.1
AC2	Well	Puit no. 59	2001	24.5	1932	6.6	231.0	102.3	61.6	3.24	96.0	255.3	741.2	8.8	0.19	3438.2	0.99	2.851	8.82E−04	−5.58	−29.75	0
AC3	River	Bou lbaz	2001	14.2	6505	7.9	257.1	54.6	2714.5	21.83	4640.0	160.2	431.8	5.0	—	14797.9	0.90	0.034	—	−5.02	−31.05	1.9
Chtouka area (Group E)																						
P9	Well	Nappe Chtouka	2000	23	1353	7.3	60	42	190	1.4	240	295	35	58.3		922	1.22	0.054		−4.87	−30.5	nd
P10	Well	Nappe Chtouka	2000	24	1074	7.5	34	21	150	1.5	89	222	75	89.9		682	2.60	0.311		−3.67	−23.8	nd
P43	Well	Nappe Chtouka	2000	24	3630	7.8	124.8	84	540	4	994	217	90	134.1		2188	0.84	0.033		−4.17	−28.1	nd
P44	Well	Nappe Chtouka	2000	20	2410	7.8	81.6	55	320	2.5	533	257	62	101		1412	0.93	0.043		−4.27	−27.8	nd
P45	Well	Nappe Chtouka	2000	25	1990	7.3	80	47	200	2.2	394	266	40	112.1		1141	0.78	0.037		−3.37	−16.9	nd
P46	Well	Nappe Chtouka	2000	23	529	7.9	28	16	68	0.5	67	181	8	5.8		374	1.57	0.044		−3.37	−16.9	nd
P47	Well	Nappe Chtouka	2000	22	1355	7.3	90.4	21	180	2.7	209	339	36	48.2		926	1.33	0.064		−4.57	−26.5	nd
P48	Well	Nappe Chtouka	2000	24	1094	7.4	67.2	35	90	1.6	138	349	12	54.9		748	1.01	0.032		−4.83	−32.1	nd
P1	Well	Nappe Chtouka	2000	25	1039	6.3	94	51	57.5	1.2	178	381	30	27.9		821	0.50	0.062		−5	−38.4	nd
P5	Well	Nappe Chtouka	2000	25	1800	7.1	126	88	86	19.1	382	315	45	24.2		1085	0.35	0.044		−6.36	−42.6	nd
P36	Well	Nappe Chtouka	2000	25	1227	7.4	92	61	78	1.6	178	366	30	27.3		834	0.68	0.062		−5.84	−38.7	nd
P40	Well	Nappe Chtouka	2000	24	1327	7.5	92	66	93.8	1.8	222	360	55	21.7		912	0.65	0.091		−6.03	−35.3	nd
P7	Well	Nappe Chtouka	2000	24	1552	7.2	106	56	92.9	2	231	386	30	26.7		931	0.62	0.048		−6	−30	nd

Table 2 Isotope data in Souss–Massa basin (results from 2001 sampling campaign)

Code	Source	Sr mg/L(mg/L)	1/Sr	$^{87}Sr/^{86}Sr$	B(mg/L)	$\delta^{11}B$ (‰)(‰)	$\delta^{13}C$ (‰)	$A^{14}C$ (pmc)
Group A — Massa plain								
AC24	Well	1.1	0.91	0.711313	0.56	44.6		
AC60	borehole	0.37	2.74	0.710595	0.05		−9.71	73.4
AC61	Borehole	0.62	1.62	0.710266	0.21		−9.39	47.8
AC33	Spring	0.49	2.02	0.710263	0.06			
Group B — Lower Souss plain								
AC43	Borehole	3.16	0.32	0.708705	2.57	41.1	−8.76	43.4
AC44	Borehole	5.77	0.17	0.70851	0.32	43.7	−9.23	56.8
AC46	Borehole	0.68	1.48	0.708794	0.07			
AC50	Borehole	0.95	1.06	0.709622	0.11			
AC58	Borehole	1.02	0.98	0.709406	0.25	43	−9.25	42.5
AC59	Borehole	0.73	1.37	0.70948	0.14			
AC47	Borehole	3.56	0.28	0.707659	0.36	12	−1.76	1.4
AC49	Borehole	0.9	1.11	0.709112	0.10			
Group C — Middle Souss plain								
AC6	Well	0.87	1.15	0.709436	0.14	37.1	−6.44	51.2
AC7	Wel	0.97	1.03	0.70976	0.14			
AC8	Wel	0.52	1.92	0.709778	0.05			
AC9	Wel	1.07	0.94	0.710131	0.13	42.8	−9.96	69.2
Group D — Upper Souss plain								
AC14	Well						−9.46	93.3
AC21	Well						−6.9	52.9
AC16	Well						−8.47	77.0
AC18	Well						−8.34	52.4
Group E — High Atlas outlet								
AC1	Spring	13	0.08	0.707629	0.13	14.6		
AC2	Well	5.27	0.19	0.707679	0.08	21.1	−8.92	58.9
AC3	River	4.58	0.22	0.711385	0.51	25.9	−9.39	86.0

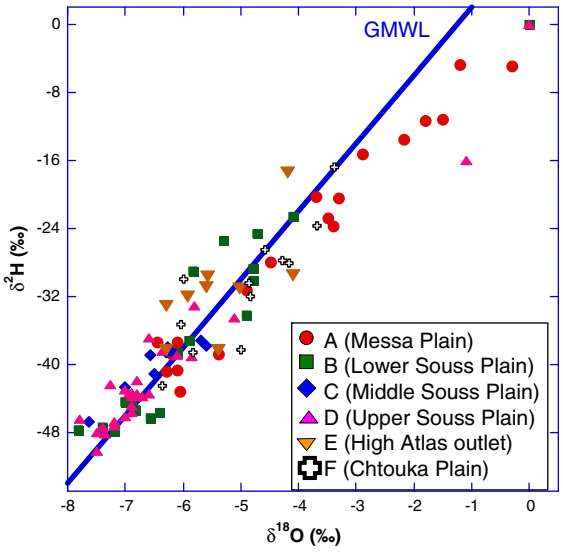

Figure 4 δ^2H vs. $\delta^{18}O$ values of groundwater and surface water investigated in this study as compared to the global meteoric water line (GMWL; Craig, 1961). Samples are sorted according by geographical distributions.

zation in these areas. This conclusion is reinforced also by isotopic evidences (see Section ''Isotopic characteristics'').

In the Messa Plain, we observed however good correlation between nitrate content and salinity (Fig. 6C) as well as positive correlations between nitrate and chloride contents and $\delta^{18}O$ values (Fig. 5). These correlations could indicate that the rise of the salinity is derived from rather evaporated agricultural return flow. In only two samples (AC24, AC34) the high salinity is associated with low nitrate concentrations, which clearly indicates that the salinity is derived from seawater intrusion.

In contrast, inland saline river water and groundwater with high Cl/TDS ratios that are identified in the high Atlas outlet (AC3, AC5; Fig. 3) are characterized by Na/Cl−1 and have conspicuously low SO_4/Cl, Br/Cl and B/Cl ratios (Table 1). These chemical characteristics are typical of halite dissolution. In fact the extremely high salinity measured in surface water at the Boulbaz point (AC3, TDS of 37,400 sampled during low water flow and 8300 mg/L during high water flow) reflects direct input of halite dissolution. The location of these samples at the southern part of the high Atlas mountains, indicates that the evaporite source is located in the sedimentary sequence of the high Atlas mountains, mainly from the Triassic evaporates. It has been shown that the southern part of the Atlas mountains contains several evaporitic formations, particularly in the Issen Basin with alteration of halite and gypsum minerals (Boutaleb et al., 2000). The chemical variations observed in

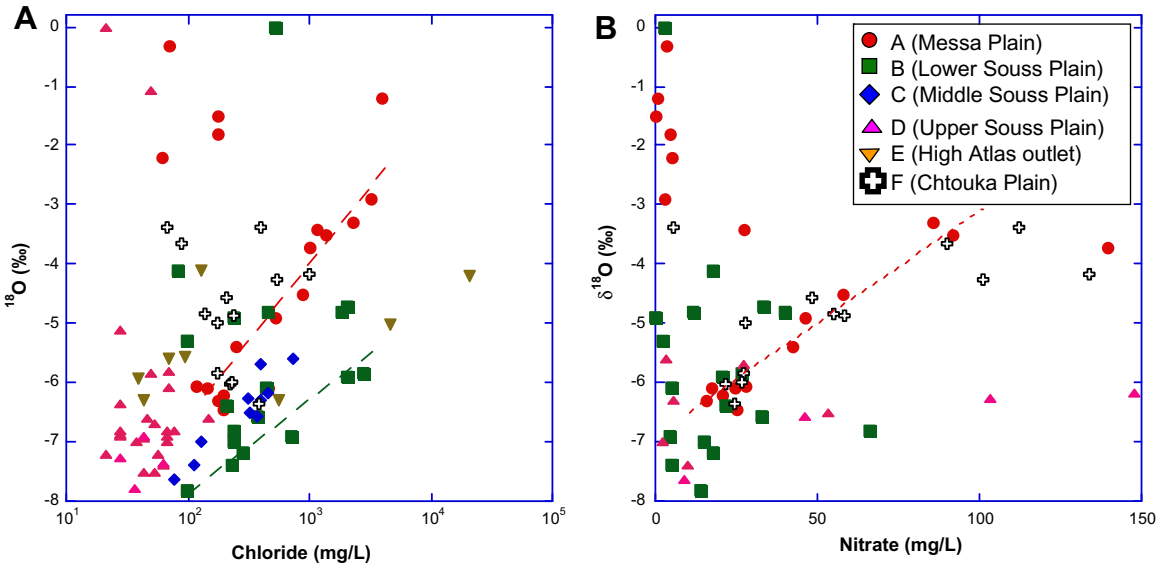

Figure 5 Variations of $\delta^{18}O$ values (‰) vs. chloride concentrations (A), and $\delta^{18}O$ values (‰) vs. nitrate concentrations (B) of groundwater and surface water investigated in this study. Samples are sorted according by geographical distributions.

groundwater from the middle Souss plain (Fig. 6A–C) may suggest that salinization of groundwater in this region is controlled by mixing with this saline source and with the sulfate-rich saline source with low Cl/TDS and high SO_4/TDS ratios. However, only in one saline sample (AC11; Cl—750 mg/L) the Br/Cl is low (3×10^{-4}) and similar to the conspicuously low Br/Cl (5×10^{-4}) of the water from a dam on the Triassic basin that characterizes this saline end-member (Fig. 7). In most of the groundwater from the middle Souss plain the Br/Cl ratios are significantly higher (2×10^{-3} to 4.6×10^{-3}), which excludes this saline source from being the predominant salinity source in the middle Souss plain. The geochemical data suggest that this saline source would have low Cl/TDS and high Br/Cl ratios.

High SO_4/TDS type water. A different saline source is identified in the high Atlas outlet with distinctively high SO_4/TDS and Ca/TDS ratios. The predominance of Ca and SO_4 ions with Ca/SO_4 ratios ~1 suggests that these waters (AC1, AC2) are derived from dissolution of gypsum minerals, possibly in the Jurassic formations of high Atlas mountains.

High NO_3/TDS type water. A large number of wells from the Massa, Chtouka, lower and upper Souss plains have high nitrate concentrations that contribute to the overall salinity of the water (Fig. 6C). In several wells the Br/Cl ratios are higher than the marine ratios (molar ratio = 1.5×10^{-3}). This suggests that bromide might be derived from application of methyl bromide pesticides (Ahkouk, 2004) that can be converted to inorganic bromide.

Isotopic characteristics

In order to provide further constraints for the salinity sources that affect the quality of groundwater in the Massa—Souss basin, we have investigated the isotopic variations of oxygen, hydrogen, strontium, and boron. The discussion below presents the results of each isotope systems in the frameworks of chemical characteristics and geographical distribution (Fig. 3).

Oxygen and hydrogen isotopes

As shown earlier, the variations of $\delta^{18}O$ and $\delta^{2}H$ values in fresh water are determined by the recharge regimes. In saline and contaminated groundwater however, the variations of $\delta^{18}O$ and $\delta^{2}H$ values are controlled also by the composition of the saline and/or contaminant sources. In all of the sub-basins, we have observed an increase of $\delta^{18}O$ values with chloride contents (Fig. 5A), thus reflecting the enriched ^{18}O characteristics of the saline sources. Along the coast, our data show that saline groundwater from the Massa and Lower Souss plains have both high $\delta^{18}O$ and marine Br/Cl ratios (Fig. 7). Given these combined geochemical and isotopic signals, these groundwater samples AC24, AC25, AC26, AC27, and AC28 from the Massa Plain, and AC 43 and AC 44 from the Lower Souss plain are derived from a saline source with chemical characteristics that mimic those of sea water intrusion ($\delta^{18}O$—0‰; Br/Cl—1.5×10^{-3}). The saline samples from the lower Souss plain are located on the coast (Fig. 3) and associated with modern seawater intrusion. In contrast, the saline samples from the Massa Plain are located far inland and are not associated with modern seawater intrusion. Some of these samples (AC24, AC26, AC27) have both high chloride and nitrate concentrations (>100 mg/L), thus the high $\delta^{18}O$ values and salinity might reflect massive evaporation and salinization of agricultural return flows. These anthropogenic signals are not accompanied by any other geochemical tracers as these saline waters have a seawater-like composition. We conclude that TDS of saline waters from the Massa Plain could be derived from surface evaporation and recycling of agricultural return flow, but we cannot exclude other saline sources, such as fossil seawater intrusion that was entrapped in this part of the basin. In the Chtouka and upper Souss plains, however, the correlation between nitrate and $\delta^{18}O$ (Fig. 5B) without corresponding chloride in-

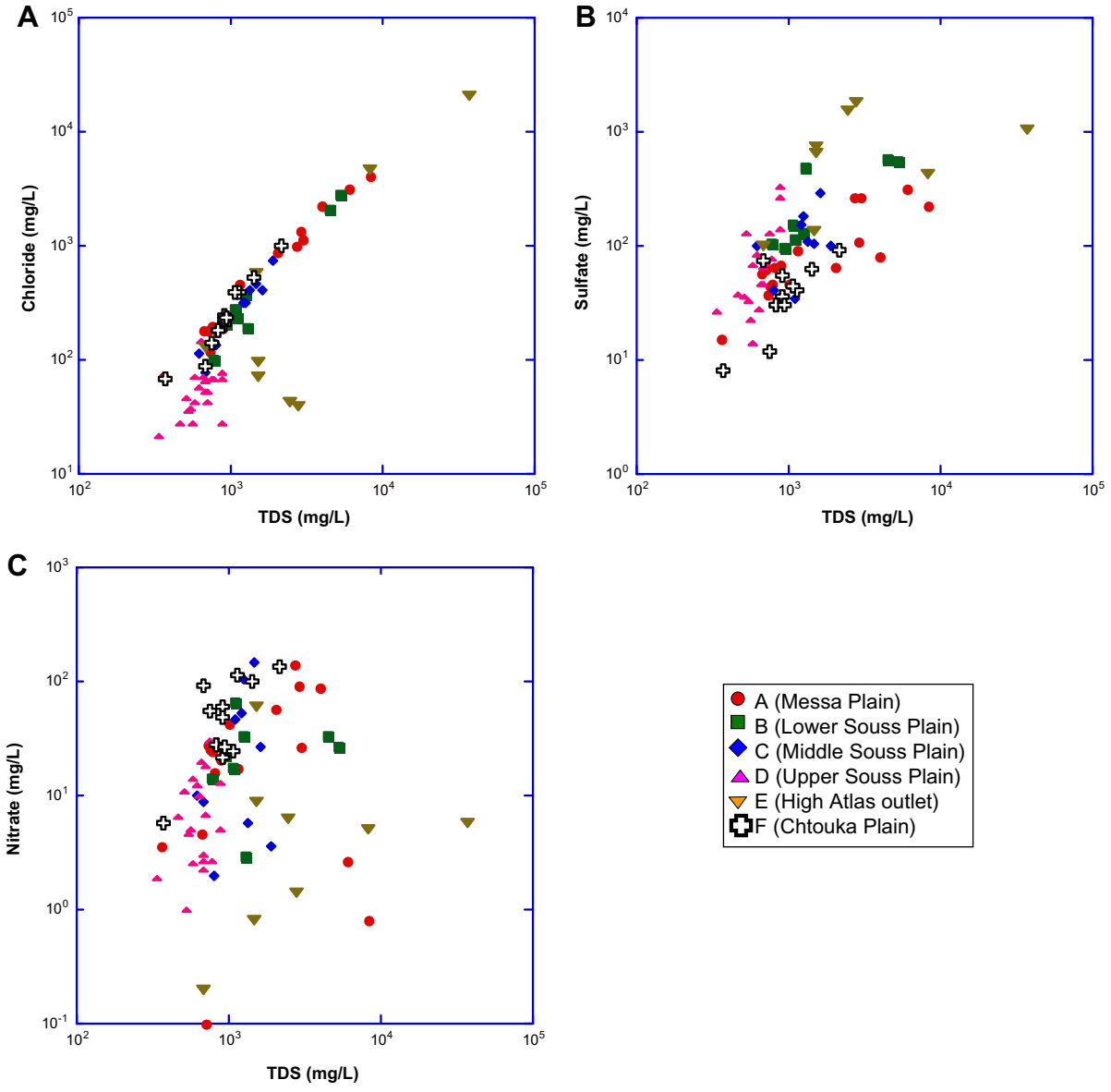

Figure 6 Variations of chloride (A), sulfate (B), and nitrate (C) concentrations (mg/L) vs. total dissolved solids (TDS mg/L) of groundwater and surface water investigated in this study. Samples are sorted according by geographical distributions.

crease suggests net contribution of agricultural return flows.

In the middle Souss Plain we observed an increase of $\delta^{18}O$ with chloride content (Fig. 5A). This increase suggests that the salinity sources in this area also have high $\delta^{18}O$ values. It should be noted that the combined $\delta^{18}O$ and Br/Cl data enable discrimination of two saline sources (1) saline source with high $\delta^{18}O$ and low Br/Cl that is identified to the external source from the high Atlas outlet (AC3); and (2) saline source with high $\delta^{18}O$ and Br/Cl ratios, which is different from any of the external saline sources in the high Atlas outlet and may represent remnants of evaporated seawater with high $\delta^{18}O$ and Br/Cl signals (Fig. 7B). This saline water could be flushed from low-conductive parts in the aquifer.

Strontium isotopes

The linear correlation between Ca and Sr contents in the investigated groundwater (Fig. 8A) indicates that Sr is a good proxy for Ca variations and sources. The variations of $^{87}Sr/^{86}Sr$ with Ca (and Sr) contents (Fig. 8B) enabled us to delineate different saline sources. In the coastal areas we observed two opposite trends: (1) high Ca with high $^{87}Sr/^{86}Sr$ ratios (up to 0.7113 in the Massa plain); and (2) high Ca with low $^{87}Sr/^{86}Sr$ ratios (as low as 0.7085 in the lower Souss plain). We suggest that the increase of Ca (and Sr) is derived from base-exchange reactions that are typically associated with seawater intrusion into coastal aquifers. The Sr isotope variations reflect release of Sr in the host aquifer sediments (Vengosh et al., 2002). The data suggest that base-exchange reactions in the Massa plains involved interaction with high $^{87}Sr/^{86}Sr$ sediments. We propose that these sediments were derived from drainage of the anti-Atlas mountains, which are composed primarily by silicate-rich igneous rocks (e.g., granite) with presumably high $^{87}Sr/^{86}Sr$ ratios that characterize such rocks (e.g., Harrington and Herczeg, 2003; Koepnick et al., 1985; Blum et al., 1994; Naftz

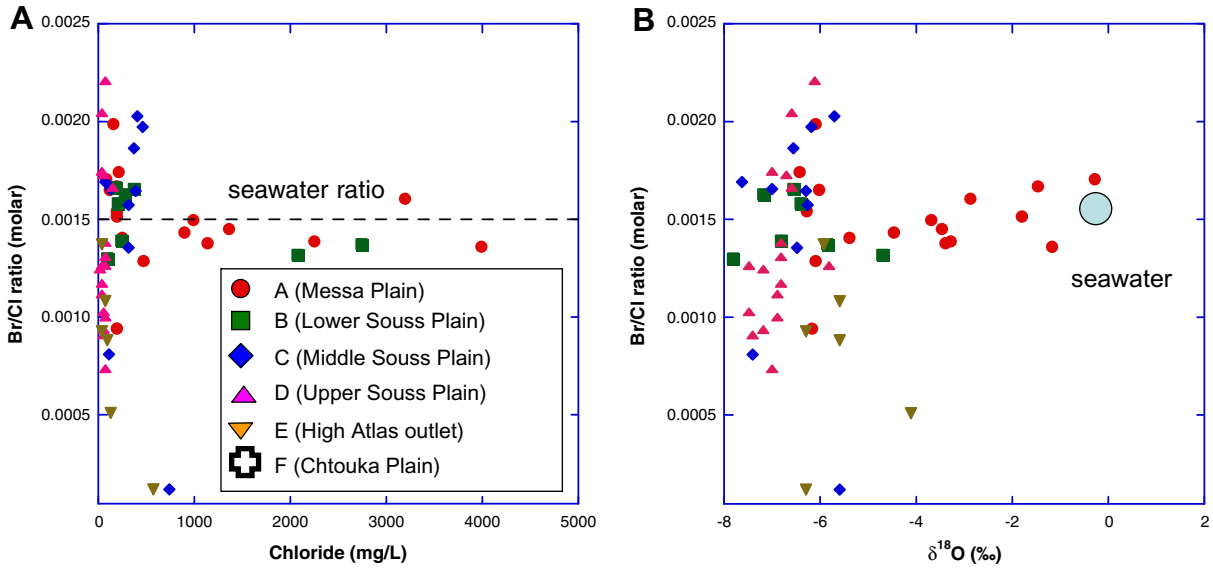

Figure 7 Br/Cl ratio (in molar units) vs. chloride concentrations (mg/L) (A) and $\delta^{18}O$ values (B) of groundwater and surface water investigated in this study. Samples are sorted according by geographical distributions.

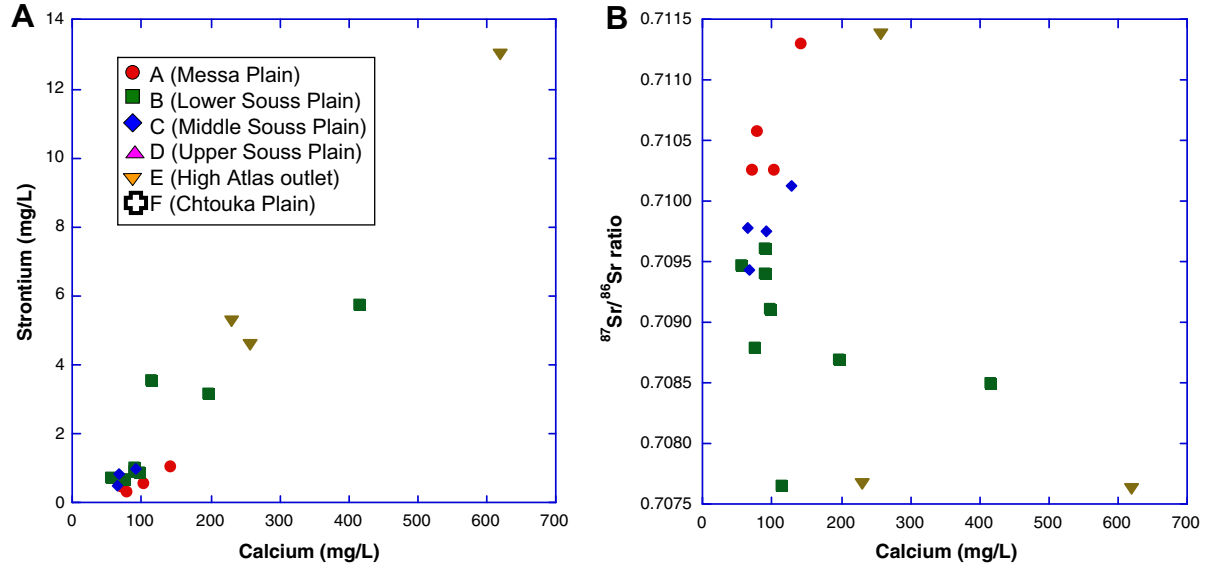

Figure 8 Variations of strontium vs. calcium concentrations (mg/L); (A) and $^{87}Sr/^{86}Sr$ ratios vs. calcium concentrations (B) in groundwater and surface water investigated in this study. Samples are sorted according by geographical distributions.

et al., 1997; Probst et al., 2000; Négrel et al., 2001; Négrel and Petelet-Giraud, 2005; Swarzenski et al., 2001; Peterman and Wallin, 1999). In contrast, the sediments in the lower Souss plains are derived from drainage of the sedimentary rocks from the high Atlas mountains with significantly lower $^{87}Sr/^{86}Sr$ ratios. Thus base-exchange reactions with these sediments result in Ca-rich water with lower $^{87}Sr/^{86}Sr$ ratios.

The high Atlas outlet saline water results from different saline sources; (1) the chloride-rich saline end-member with high Cl/TDS ratios (AC3) has a high $^{87}Sr/^{86}Sr$ ratio (0.7114); and (2) the sulfate-rich saline source with low Cl/TDS ratios (AC1, AC2) has a low $^{87}Sr/^{86}Sr$ ratio (0.7076). We propose that these isotopic signals reflect the origin of the saline sources. Secular variations of $^{87}Sr/^{86}Sr$ ratios in seawater through time are recorded in marine evaporites since Sr isotopes are not fractionated during mineral precipitation from seawater. Likewise, dissolution, for example, of sulfate minerals by groundwater would not modify the original $^{87}Sr/^{86}Sr$ ratio signature. During the late Triassic or Liass, seawater had an $^{87}Sr/^{86}Sr$ ratio signature of ~0.7076 (Burke et al., 1982; Korte et al., 2003; Veizer and Compston, 1974; Veizer et al., 1997, 1999). This value is identical to the sulfate-rich saline water (AC1, AC2) and confirms that this saline source is originated from dissolution of late Triassic or Liassic gyp-

sum. In contrast, the high $^{87}Sr/^{86}Sr$ ratio (0.7114) measured in the other saline source from the high Atlas outlet is significantly higher than the $^{87}Sr/^{86}Sr$ record of any sedimentary rocks along the Phanerozoic (Veizer et al., 1997, 1999), and thus indicate that this saline source is derived from interactions with silicate rocks.

It should be noted that the saline water in the middle Souss plains (samples AC6, AC7, AC8, AC9) has high $^{87}Sr/^{86}Sr$ ratios (0.7095 to 0.7101), which is different from the sulfate-rich source with lower $^{87}Sr/^{86}Sr$ ratios. This observation is consistent with relatively high Br/Cl ratios that characterize this water type. Some samples (AC6, AC9, AC24) are characterized by both high nitrate and $^{87}Sr/^{86}Sr$ ratios. One would suggest that the Sr isotope composition is also masked by anthropogenic impact (e.g., fertilizers). Previous studies have shown that anthropogenic contributions through agricultural activity induces an input of Sr that may modify the original Sr isotopes of the water (Böhlke and Horan, 2000; Négrel and Deschamps, 1996; Négrel et al., 2001; Négrel and Petelet-Giraud, 2005). The nitrate-rich groundwater in our study have high $^{87}Sr/^{86}Sr$ ratios of >0.7095, which could reflect the nature of the fertilizers used in the study area.

Finally groundwater from the Cretaceous (Turonian) confined aquifer (AC47), is characterized by low $^{87}Sr/^{86}Sr$ ratios of 0.70766. This ratio corresponds to the $^{87}Sr/^{86}Sr$ ratio of Turonian seawater (Veizer et al., 1997) and thus indicates that most of the Sr in that water is derived from water-rock interaction with the carbonate aquifer rocks. The low $^{87}Sr/^{86}Sr$ of the deep groundwater is different from the typically high $^{87}Sr/^{86}Sr$ in groundwater from the lower Souss Plain, and thus provides a useful tool to delineate water sources in that part of the aquifer.

Boron isotopes

The relationship between B and Cl contents (Fig. 9A) provides an evaluation of the relative enrichment of boron in the water. The combination of B/Cl and boron isotopic ratios (expressed as $\delta^{11}B$ values) provides a useful tool to delineate the sources of groundwater contamination (Vengosh et al., 1994, 1998, 2005; Bassett, 1990; Bassett et al., 1995; Davidson and Bassett, 1993; Eisenhut et al., 1996; Eisenhut and Heumann, 1997) and sources of salinity (Vengosh et al., 1992). Seawater has a distinguished boron isotopic composition ($\delta^{11}B = 39‰$) while non-marine saline sources and anthropogenic effluents (e.g., sewage, $\delta^{11}B = 10‰$) have significantly lower $\delta^{11}B$ values. Our data (Fig. 9B) show that coastal groundwater from the Massa (AC 24) and Lower Souss (AC 43, AC44, AC58) plains have typically high $\delta^{11}B$ values (>39‰) that is consistent with the isotopic composition that is expected for seawater intrusion (Vengosh et al., 1994). In contrast, groundwater from the Cretaceous (Turonian) confined aquifer (AC47) is characterized by low $\delta^{11}B$ (12‰) value and relatively high B/Cl ratio (6.4×10^{-3}) that are different from the composition of seawater intrusion. Given the low $A^{14}C$ (see below) and low $^{87}Sr/^{86}Sr$ ratios, we relate this composition to water-rock interactions with the host carbonate rocks in the confined aquifer. Indeed, low $\delta^{11}B$ values were also reported in groundwater from a similar Turonian aquifer (Judea Group) in Israel (Vengosh et al., 1991).

The high Atlas outlet saline waters yield different boron isotopic signals; sulfate-rich water of AC1 has a $\delta^{11}B$ value of 15‰ and very high B/Cl ratio, whereas the chloride-rich saline water (AC2, AC3) has higher $\delta^{11}B$ values of 20–25‰. This composition is consistent with the isotopic composition expected for marine gypsum given the isotopic fractionation between evaporated seawater and marine evaporates (Vengosh et al., 1992). This is also consistent with the Sr isotopic signal that suggest dissolution of sedimentary Triassic gypsum. In contrast, the lower $\delta^{11}B$ value of the Cl-rich water suggests contribution of silicate rock with typically lower $\delta^{11}B$ signal (~0‰). Once again, this is consistent with the extremely high $^{87}Sr/^{86}Sr$ ratio of this saline source. As

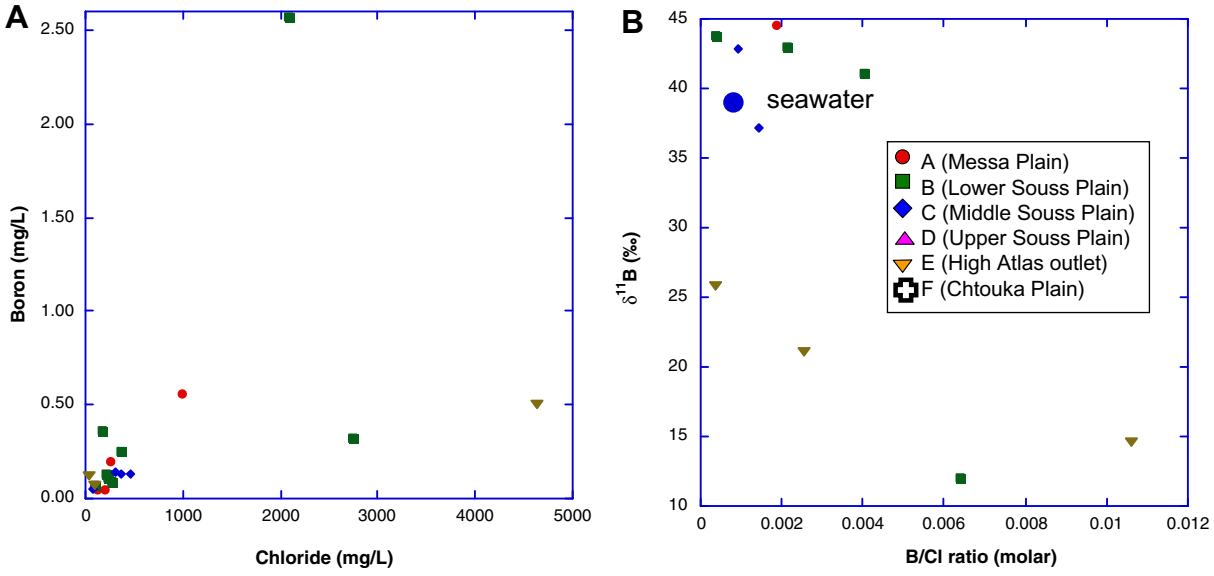

Figure 9 Variations of boron vs. chloride concentrations (mg/L); (A) and $\delta^{11}B$ values (‰) vs. B/Cl ratios (molar units) (B) in groundwater and surface water investigated in this study. Samples are sorted according by geographical distributions.

shown for other geochemical and isotopic parameters, the boron isotopic composition of the saline groundwater from the middle Souss plain (AC6 and AC9) is not similar to either of these saline sources. Instead, the relatively high $\delta^{11}B$ values of these samples (37‰ and 43‰) are consistent with the composition expected for remnants of evaporated seawater. This corresponds to the relatively high Br/Cl ratios of these samples that suggest origin from early stages of evaporated seawater.

Water residence time

In order to facilitate a sustainable water resource management program for the Souss–Massa aquifer system, it is desirable to delineate the residence time of the water (i.e., modern vs. old water; Schlosser et al., 1988; Mook, 1980; Michel, 2005; Plummer, 2005), differentiate between modern and ancient seawater intrusions (Yechieli et al., 2001; Sivan et al., 2005), and to distinguish between modern seawater intrusion and entrapped formation water. The residence times of the investigated waters in the aquifer may hold also the key for evaluating their origins.

Tritium

The tritium data from the Souss–Massa aquifer basin show very low values ranging from 0 to 5.5 TU (Fig. 10). A large number of the groundwater samples, 26 out of 61 samples has tritium level of zero, and 42 samples (~70%) have tritium levels below 1 TU. The higher values were observed in surface waters AC19 (5.5 TU) and AC23 (3 TU). Since tritium activities in precipitation in the region are not known, we used the surface water tritium signature as a representative of modern meteoric signal, in the range of 5–10 TU (IAEA//WMO, 2004). As the water recharges vertically within the basin and laterally from the recharge zone adjacent to the aquifer basins, the tritium activities are expected to decrease with time. In contrast to the surface water, most of the groundwater samples have very low, mostly zero tritium levels, which indicate that both the vertical and lateral recharge process are longer than about 30 years. The lack of high tritium activities in groundwater suggests that the 1960's tritium peak (Schlosser et al., 1988; Mook, 1980; Michel, 2005; Plummer, 2005; Yechieli et al., 2001) has already diminished in that groundwater system. Alternatively, if all groundwater samples were very young (of the last decade), one would expect to have tritium levels similar to those measured in the surface waters.

In the Massa Plain, we observed an inverse correlation between $\delta^{18}O$, NO_3 and tritium (Fig. 10). This reflects the mixture between ^{18}O-enriched and young surface water, derived primarily from recharge in the anti-Atlas mountains (marked as AA in Fig. 10) and deep older groundwater with lower $\delta^{18}O$ values. In contrast, recharge on the eastern side of upper Souss basin (HA in Fig. 10) is characterized by high tritium and low $\delta^{18}O$ values, reflecting less evaporation of surface water in that part of the recharge zone of the aquifer (Fig. 3).

It is interesting to note that some of the saline waters have measurable tritium levels. In the high Atlas outlet, the saline water (AC1 and AC3) has tritium activities of 3 and 2 TU, respectively, which indicates that the salts (NaCl for AC1 and $CaSO_4$ for AC3) were dissolved by young meteoric water. In the coastal areas, saline waters from the Massa Plain (AC24; Cl = 1000 mg/L) and Lower Souss Plains (AC 44; Cl = 2750 mg/L) have tritium activities of 1.7 and 0.3 TU, respectively. Saline groundwater from the coastal aquifer of Israel with salinity level identical to seawater has tritium range of 2–3 TU (Sivan et al., 2005). Given that seawater in the mid-1960s had tritium peak of about 38 TU (Roether and Schiltzer, 1991) the tritium range measured in the Israeli coast corresponds to seawater penetration inland between the mid-1960s and the mid-1980s (Sivan et al., 2005). Consequently, the values measured in the Massa and Low Souss basins reflect relatively modern seawater

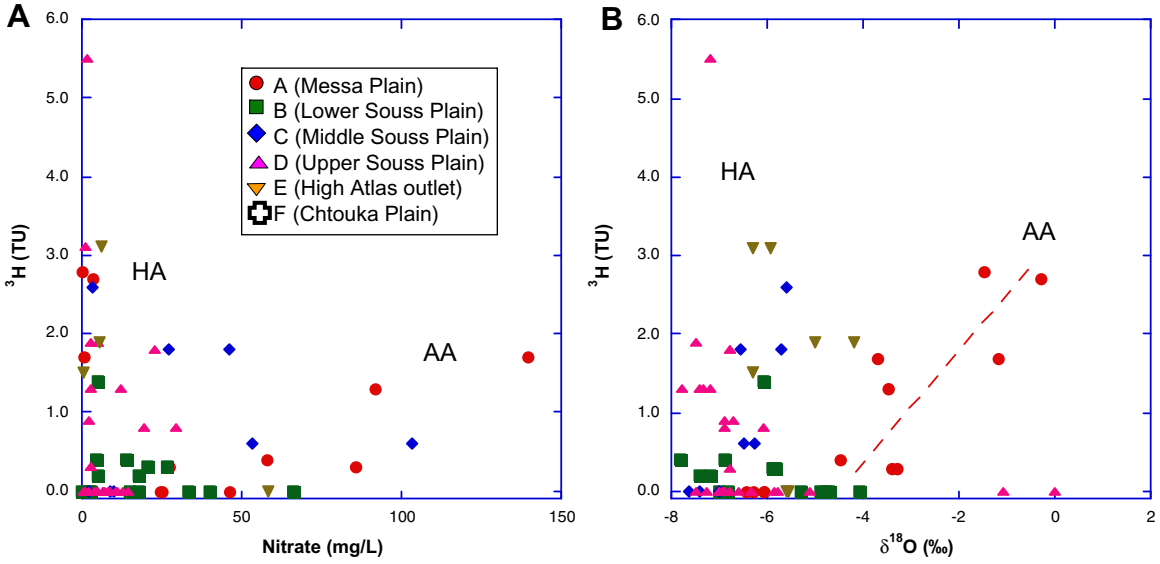

Figure 10 Tritium (TU) vs. nitrate concentrations (mg/L); (A) and $\delta^{18}O$ values (‰); (B) in groundwater and surface water investigated in this study. Samples are sorted according by geographical distributions.

intrusion. In the fresh water-seawater mixture, it seems that the freshwater component has a lower tritium content, which reduces the overall tritium activity of the saline groundwater.

Carbon-14

Carbon-isotopic measurements (^{14}C and $\delta^{13}C$) on dissolved inorganic carbon (DIC, mainly HCO_3) were used to provide information on the relative ages of the ground water pumped from fourteen points within the basin. The $\delta^{13}C$ values vary between $-9.96‰$ and $-1.76‰$ vs. PDB with an average of $-8.74 \pm 1.1‰$. This range suggests that DIC in the system is derived from: (i) dissolution of limestone/dolostone in the Atlas Mountains ($\delta^{13}C = 0‰$) and (ii) conversion of soil CO_2 ($\delta^{13}C = -25‰$) to bicarbonate (Mook, 1980; Salomons and Mook, 1986; Fontes, 1992; Douglas et al., 2006; Mahlknecht et al., 2006). The ^{14}C activities range from 1.35 to 93.3 pmc (Table 2). Sample AC47, which represents the Cretaceous confined aquifer, displays the lowest values of $\delta^{13}C$ and $A^{14}C$; $-1.76‰$ and 1.35 pmc, respectively. This enriched ^{13}C and low $A^{14}C$ values can be explained by massive interaction with old carbonate rocks in this confined aquifer, where the influence of renewable soil CO_2 is negligible (Grassi and Cortecci, 2005).

We used the stable carbon isotopes as an indicator for the degree of carbon ''dilution'' by water–rock interactions and dissolution of old carbon from the host aquifer rocks. Given the isotopic fractionation of carbon isotopes during dissociation of hydrated CO_2 into HCO_3 (fractionation factor of about 9‰) the original $\delta^{13}C$ of soil CO_2($\sim -23‰$) is expected to be converted to DIC with $\delta^{13}C \sim -15‰$ (Clark and Fritz, 1997; Appelo and Postma, 1993). Thus, we consider two end-members; a predominant rock contribution with $\delta^{13}C_{carb} \sim 0‰$ and $A^{14}C \sim 0$ pmc, and a soil CO_2 source with $\delta^{13}C_{recharge} \sim -15‰$ and $A^{14}C \geqslant 100$ pmc. In a such system, the dilution factor, q, depends on the mixing ratios between the different end-members (Clark and Fritz, 1997):

$$q = (\delta^{13}C_{DIC} - \delta^{13}C_{carb})/(\delta^{13}C_{recharge} - \delta^{13}C_{carb}) \quad (1)$$

where $\delta^{13}C_{DIC}$ is the measured $\delta^{13}C$ in groundwater. Fig. 11 presents the variations of $\delta^{13}C$ and $A^{14}C$ values. The data show that some of the samples lie on a mixing line between the carbonate rock end-member and a recharge source with $\delta^{13}C_{recharge} \sim -15‰$ and $A^{14}C \sim 130$ pmc. In order to calculate the apparent age of the groundwater, we use the decay equation of ^{14}C corrected for two different models. In the first model, we used q values obtained from the mixing of $\delta^{13}C$ end-members (Eq. (1)) to correct for ''carbonate dilution''. In the second model, we used the combined mixing of $\delta^{13}C$ and $A^{14}C$ (Line A in Fig. 11) to estimate the initial values of ^{14}C that correspond to the measured $\delta^{13}C$ values. We calculated the relative deviation of the measured ^{14}C activities from the expected initial values along the mixing line. For the two models we assume a closed system condition in which no renewable DIC is recharged from the unsaturated zone. This assumption is justified given the low, mostly zero, activities of tritium in the water. According to the first and second models, most of the groundwater yields an apparent age range of 3.5–7 Kys BP and modern to 4 Kys BP, respectively (Table 3). The only exception is sample AC47, which represents the Cretaceous (Turonian) confined aquifer ($A^{14}C = 1.35$ pmc) with calculated ages of

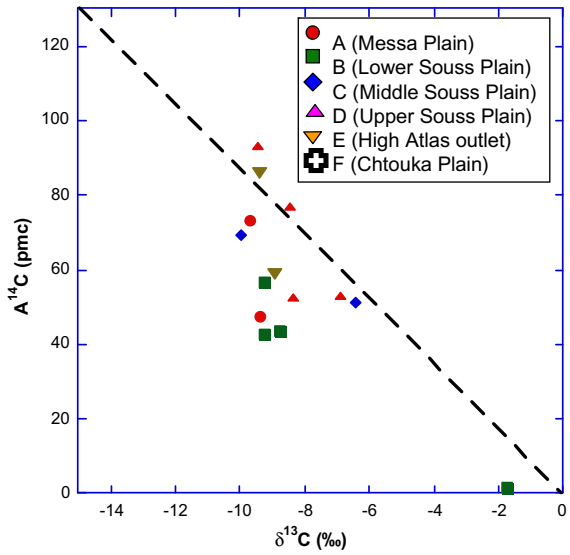

Figure 11 $A^{14}C$ (activity of ^{14}C normalized to per-cent modern carbon; pmc) vs. $\delta^{13}C$ values (‰) in groundwater and surface water investigated in this study. Samples are sorted according by geographical distributions. Line A represents a theoretical closed system mixing between modern DIC (derived from soil CO_2 with $A^{14}C$–130 pmc and $\delta^{13}C \sim -15‰$) and marine carbonate rock DIC ($A^{14}C$–0 pmc and $\delta^{13}C$–0‰). Groundwater samples with $A^{14}C$ and $\delta^{13}C$ values along this line are hypothesized to reflect mixing between soil-derived DIC and carbonate rock dissolution under a closed system and thus are modern, whereas deviation from that mixing line is modeled to ^{14}C decay and thus residence time of the groundwater.

Table 3 Carbon isotopes data and residence time calculations according to (1) $\delta^{13}C$ mixing model; and (2) Combined $A^{14}C$ and $\delta^{13}C$ mixing model, derived from Line A in Fig. 11 (see text for details)

Sample ID	$\delta^{13}C$ (‰)	$A^{14}C$ (pmc)	q ($\delta^{13}C$)	Model 1 ages (years)	Model 2 ages (years)
AC60	−9.71	73.4	0.65	3600	1123
AC61	−9.39	47.8	0.63	3872	4264
AC43	−8.76	43.4	0.58	4446	4633
AC44	−9.23	56.8	0.62	4019	2836
AC58	−9.25	42.5	0.62	3997	5170
AC47	−1.76	1.4	0.12	17716	19906
AC6	−6.44	51.2	0.43	6991	734
AC9	−9.96	69.2	0.66	3385	1800
AC14	−9.46	93.3	0.63	3812	0
AC21	−6.9	52.9	0.46	6420	1035
AC16	−8.47	77.0	0.56	4726	0
AC18	−8.34	52.4	0.56	4853	2628
AC2	−8.92	58.9	0.59	4298	2322
AC3	−9.39	86.0	0.63	3872	0

18 and 20 Kys BP, according to the first and second models, respectively. This indicates that water derived from this deep confined aquifer was recharged during the late Pleistocene. In contrast, most of the investigated groundwater yielded apparent ages of modern to a few thousands of

years. According to the second model, groundwater samples that represent recharge water from the upper and middle Souss Plain and from the high Atlas have typical young ages of modern to 2 Kys BP years, whereas groundwater from the lower Souss and Massa plain on the coast have apparent older ages of 2–5 Kys BP. This observation is also consistent with tritium data (Tables 2 and 3). In the coastal area, the apparent older age estimates are for both fresh and saline groundwater (e.g., AC44 and AC 43) since most of the DIC in the fresh-saline mixture is derived from the fresh water component. Likewise, the high saline water from the high Atlas outlet (AC3) has modern ^{14}C age, which is also consistent with the high tritium activities in this sample. We conclude that modern recharge of groundwater occurs along the eastern and northern sections of the Souss Basin while groundwater along down-gradient flow paths, in the Lower Souss basin and Massa Plain (Fig. 3), are older and thus reflecting modern recharge and/or recharge during the Holocene (<6 Kys BP).

Conclusions

This study presents the results of several isotopic and age-dating isotopic tools in an attempt to reveal the origin of recharge water, the salinity, and the residence time of surface and groundwater resources of Souss–Massa region in western Morocco. Identification of the geochemical processes that control the salinity and evolution of the groundwater is essential for predicting the long-term variations in groundwater quality in the Souss–Massa aquifer system. The data revealed a complex hydrogeological system in which several sources of salinity have been identified:

(1) Sea water intrusion along the coastal areas of Massa and Lower Souss basins, characterized by high Cl/TDS, low Na/Cl and SO_4/Cl, marine Br/Cl ($\sim 1.5 \times 10^{-3}$), and marine $\delta^{11}B$ ($\sim 40‰$) and high $\delta^{18}O$ and $\delta^{2}H$ values. In the Massa basin, base-exchange reactions with aquifer sediments have extracted Sr with high $^{87}Sr/^{86}Sr$ ratios (up to 0.7113) whereas similar water-rock interaction in the lower Souss basin yielded lower $^{87}Sr/^{86}Sr$ ratios (as low as 0.7085). We relate these differences to different sediment inputs; contribution of sediments from weathering of silicate rocks in the anti-Atlas mountains in the south relative to weathering of carbonate rocks from the high Atlas mountains with lower $^{87}Sr/^{86}Sr$ ratios in the north.

(2) Recycling of agricultural return flows in the aquifer as reflected by the high nitrate concentrations (up to 150 mg/L) and high $\delta^{18}O$ and $\delta^{2}H$ values. In some cases (e.g., the Massa plain), salinization by old seawater intrusion is coinciding with anthropogenic contamination.

(3) Dissolution of evaporites along the outcrops of the high Atals mountains in the northern part of the basin. Two types of evaporite dissolution are identified:

(i) NaCl type with high Cl/TDS and Na/Cl, low Br/Cl and B/Cl, low $\delta^{11}B$ (15‰) and high $^{87}Sr/^{86}Sr$ ratio (0.7114) that reflect dissolution of halite minerals.

(ii) $CaSO_4$ type with low Cl/TDS, high SO_4/Cl, Na/Cl, B/Cl, low $\delta^{11}B$ (20–25‰) and low $^{87}Sr/^{86}Sr$ (0.7076) ratios that reflect dissolution of Late Triassic or earlier Liassic gypsum deposits.

(4) Mixing with entrapped residual evaporated seawater in the middle Souss Basin with relatively high Br/Cl ($\sim 2 \times 10^{-3}$), high $\delta^{11}B$ ($\sim$37 and 43‰), and high $^{87}Sr/^{86}Sr$ ratio (0.7095 to 0.7101).

The stable isotopes data indicate that the Souss–Massa shallow aquifer is highly influenced by the contribution of recharge water from the high Atlas mountains that has a high rainfall, particularly in its upstream part along the upper Souss plain. The data indicate that the high Atlas mountains constitute the main recharge area of the Souss–Massa shallow aquifer. In addition, tritium and ^{14}C data revealed modern groundwater in the recharge zones of the aquifer, while deep groundwater in the confined and down-flow parts of the aquifer are older and reflect past recharge during the Holocene. The results of age estimates based on ^{3}H and ^{14}C data suggested that relatively old groundwater is practically mined at some wells. This indicates that the Souss–Massa basin is very vulnerable to contamination process, and the rates of salinization (e.g., seawater intrusion) or anthropogenic contamination (recycling of agricultural return flow) are faster than natural replenishment of the aquifer. We distinguish between two major areas in the basin: (i) the Souss upstream part with a high water quality and modern recharge, and (ii) the downstream coastal areas with low water quality derived from different salinity sources and long residence time of groundwater. Obviously, continued water utilization in the coastal and near-coastal areas would further increase the depletion of water resource and degradation of groundwater quality. These factors should take into consideration in future water management plans; decrease pumping from the more vulnerable and contaminated coastal groundwater and further exploration of the high quality and renewable water resources in the upper zone of the Souss Basin. Moreover, the results of this study indicate that future exploration of the deep groundwater from the Cretaceous (Turonian) confined aquifer would result in production of good quality water but with very old ages ($\sim$20 Kys BP), which infers exploitation of non-renewable water resource.

Acknowledgement

We are grateful for the help by all laboratories where all analyses were made. The research has been carried out as part of the Coordinated Research Projects (CRP) of the International Atomic Energy Agency (IAEA). The authors thank Dr. Aggarwal and all the staff of Isotopic Hydrology section at IAEA (Vienna, Austria) for the facilities provided during the research contract numbers F33012 and 12893. Furthermore, we thank the Hydraulic Agency of Souss–Massa Basin (Agadir), CNESTEN (Rabat) and Livermore National Laboratory (California, USA) for their collaboration. We also would like to thank Dr. W.M. Edmunds for his comments and critical evaluation for improving the final project report, which consequently led to the development of this

research. We also want to express our sincere thanks to J. Mudry and B. Ekwurzel for their helpful comments and suggestions at various stages of this research project. Finally, we thank two anonymous reviewers and the editor for constructive comments that improved this article.

References

Ahkouk, S., Hsissou, H., Bouchaou, L., Krimissa, M., Mania, J., 2003. Impact des fertilisants agricoles et du mode d'irrigation sur la qualité des eaux souterraines (cas de la nappe des Chtoukas, bassin du Souss—Massa). Afr. Geosci. Rev. 3, 4.

Ahkouk, S., 2004. Impact des fertilisants agricoles et du mode d'irrigation sur la qualité des eaux souterraines en zones irriguées sous climat semi-aride: Cas de la plaine des Chtouka, bassin du Souss—Massa, Maroc. Thèse de Doctorat. Univ. Ibn Zohr, Agadir, 161 p.

Al-Weshah, R., 2002. The role of UNESCO in sustainable water resources management in the Arab World. Desalination 152, 1—l 3.

Ambroggi, R., 1963. Etude géologique du versant méridional du Haut-Atlas occidental et de la plaine du Souss. Notes et Mém Serv Géol Maroc 157, 321.

Appelo, C.A.J., Postma, D., 1993. Geochemistry, Groundwater, and Pollution. A.A. Balkema, Rotterdam.

Bassett, R.L., 1990. A critical evaluation of the available measurements for the stable isotopes of boron. Appl. Geochem. 5, 541—554.

Bassett, R.L., Buszka, P.M., Davidson, G.R., Chong-Diaz, D., 1995. Identification of ground water solute sources using boron isotopic composition. Environ. Sci. Technol. 29, 2915—2922.

Bennetts, D.A., Webb, J.A., Stone, D.J.M., Hill, D.M., 2006. Understanding the salinisation process for groundwater in an area of south-eastern Australia, using hydrochemical and isotopic evidence. J. Hydrol. 323, 178—192.

Blum, J.D., Erel, Y., Brown, K., 1994. $^{87}Sr/^{86}Sr$ ratios of Sierra Nevada stream waters: implications for relative mineral weathering rates. Geochim. Cosmochim. Acta 58, 5019—5025.

Böhlke, J.K., Horan, M., 2000. Strontium isotope geochemistry of groundwaters and streams affected by agriculture, Locust Grove, MD. Appl. Geochem. 15, 599—609.

Bouchaou, L., Michelot, J.L., Chauve, P., Mania, J.Et., Mudry, J., 1995. Apports des isotopes stables à l'étude des modalités d'alimentation des aquifères du Tadla (Maroc) sous climat semi-aride. C.R. Acad. Sci. 320, 95—101.

Bouchaou, L., Qurtobi, M., Gaye, C.B., Hsissou, Y., Ibn Majah, M., Michelot, J.L., Marah, H., Safsaf, N., El Hamdaoui, A., 2003. Isotopic investigation of salinity and water resources in the souss—Massa basin (Morocco). International Symposium on isotope hydrology and integrated water resources management 19—23 May, 2003, Vienna, Austria.

Bouchaou, L., Hsissou, Y., Krimissa, M., Krimissa, S., Mudry, J., 2005. 2H and 18O isotopic study of ground waters under a semi-arid climate. Environmental Geochemistry, pp. 57—64; Green Chemistry and Pollutants in Ecosystems. In: Lichtfouse, E., Schwarzbauer, J., Robert, D. (Eds.), XXVI, 780 p. 289 illus. ISBN: 3-540-22860-8 Springer.

Boughriba, M.A. Melloul, Y. Zarhloule, A. Ouardi, in press. Extension spatiale de la salinisation des ressources en eau et modèle conceptuel des sources salées dans la plaine des Triffa (Maroc nord-oriental). C.R. Geosciences. Corrected Proof, Available online. http://france.elsevier.com/direct/CRAS2A.

Boutaleb, S.L., Bouchaou, J., Mudry, Y., Hsissou, J., Mania, Et., Chauve, P., 2000. Acquisition of salt mineralization in semi-arid watershed: The case of Qued Issen (Western Upper Atlas, Morocco). Hydrogeol. J. 8, 230—238.

Bullen, T.D., Krabbenhoft, D.P., Kendall, C., 1996. Kinetic and mineralogic controls on the evolution of groundwater chemistry and 87Sr/86Sr in a sandy silicate aquifer, northern Wisconsin, USA. Geochim. Cosmochim. Acta 60, 1807—1821.

Burke, W.H., Denison, R.E., Hetherington, E.A., Koepnick, R.B., Nelson, H.F., Otto, J.B., 1982. Variation of 87Sr/86Sr throughout Phanerozoic time. Geology 10, 516—519.

C.A.G. (Compagnie Africaine de géophysique). 1963. Reconnaissance par prospection électrique dans la région du Souss. Rapport DRH, Agadir.

Calvache, L.L., Pulido-Bosh, A., 1997. Effects of geology and human activity on the dynamics of salt-water intrusion in three coastal aquifers in southern Spain. Environ. Geol. 30, 215—223.

Clark, I., Fritz, P., 1997. Environmental Isotopes in Hydrogeology. Lewis Publishers, Boca Raton.

Combe, M., El Hebil, A., 1977. Vallée du Souss, in Ressources en eau du Maroc, t3. Domaines atlasique et sud-atlasique. Notes et Mémoires du Service Géologique Maroc, 231, 169—201.

Craig, H., 1957. Isotopic standards for carbon and oxygen and correction factors for mass spectrometric analyses of carbon dioxide. Geochim. Cosmochim. Acta 12, 133—149.

Craig, H., 1961. Isotope variations in meteoric waters. Science 133, 1702—1703.

Custodio, E., 1987. Hydrogeochemistry and tracers. In: Custodio E. (Ed.), Groundwater problems in coastal areas. UNESCO, Studies and Reports in Hydrology 45, 213—269.

Dijon, R., 1969. Etude hydrogéologique et inventaire des ressources en eau de la vallée du Souss. Notes et Mémoires du Service Géologique Maroc 214, 291.

Dindane, K., Bouchaou, L., Hsissou, Y., Krimissa, M., 2003. Hydrochemical and isotopic characteristics of groundwater in the Souss upstream basin, southwestern Morocco. J. Afr. Earth Sci. 36, 315—327.

Davidson, G.R., Bassett, R.L., 1993. Application of boron isotopes for identifying contaminants such as fly ash leachate in ground water. Environ. Sci. Technol. 27, 172—176.

Douglas, A., Osiensky, J.L., Kent Keller, C., 2006. Carbon-14 dating of ground water in the Palouse Basin of the Columbia river basalts. J. Hydrol. 334, 502—512.

D.R.P.E., 2004. Elements d'actualisation du plan directeur du bassin hydraulique du Souss-Massa. Rapport interne, 89p. ABHSM, Agadir.

Edmunds, W.M., Guendouz, A.H., Mamou, A., Moulla, A., Shand, P., Zouari, K., 2003. Groundwater evolution in the Continental Intercalaire Aquifer of southern Algeria and Tunisia; trace element and isotopic indicators. Appl. Geochem. 18, 805—822.

Eisenhut, S., Heumann, K.G., 1997. Identification of ground water contaminations by landfills using precise boron isotope ratio measurements with negative thermal ionization mass spectrometry. Fresenius J. Anal. Chem. 359, 371—374.

Eisenhut, S., Heumann, K.G., Vengosh, A., 1996. Determination of boron isotopic variations in aquatic systems with negative thermal ionization mass spectrometry as a tracer for anthropogenic influences. Fresenius J. Anal. Chem. 354, 903—909.

Ekwurzel, B., Moran, J.E., Hudson, G.B., Bissani, M., Blake, R., Krimissa, M., Mosleh, N., Marah, H., Safsaf, N., Hsissou, Y., Bouchaou, L., 2001. An isotopic investigation of salinity and water sources in the Souss—Massa Basin, Morocco. In: Ouazar, D., Cheng, A.H.D. (Eds.), The first international conference on salt water intrusion and coastal aquifers. Essaouira, Morocco.

Farber, E., Vengosh, A., Gavrieli, I., Marie, A., Bullen, T.D., Mayer, B., Holtzman, R., Segal, M., Shavit, U., 2004. The origin and mechanisms of salinization of the Lower Jordan River. Geochim. Cosmochim. Acta 68, 1989—2006.

Fedrigoni, L., Krimissa, M., Zouari, K., Maliki, A., Zuppi, G.M., 2001. Origin of the salinisation and hydrogeochemical behavior of a phreatic suffering severe natural and anthropic constraints

an example from the Djebeniana aquifer (Tunisia). C.R. Acad. Sci. 332, 665–671.

Fontes, J.Ch., 1992. Chemical and isotopic constraints on 14C dating of groundwater. In: Long, Taylor, Kra (Eds.), Radiocarbon After Four Decades. Springer-Verlag, New York, pp. 242–261.

Grassi, S., Cortecci, G., 2005. Hydrogeology and geochemistry of the multilayered confined aquifer of the Pisa plain (Tuscany – Central Italy). Appl. Geochem. 20, 41–54.

Harrington, G.A., Herczeg, A.L., 2003. The importance of silicate weathering of a sedimentary aquifer in arid Central Australia indicated by very high Sr-87/Sr-86 ratios. Chem. Geol. 199 (3–4), 281–292.

Hsissou, Y., Bouchaou, L., Mudry, J., Mania, P., Chauve, P., 2002. Use of chemical tracing to study acquisition modalities of the mineralization and behaviour of unconfined groundwaters under a semi-arid climate: the case of the Souss plain (Morocco). Env. Geol. 42, 672–680.

Hsissou, Y., Mudry, J., Mania, J., Bouchaou, L., Chauve, P., 1999. Utilisation du rapport Br/Cl pour déterminer l'origine de la salinité des eaux souterraines: exemple de la plaine du Souss (Maroc). C.R. Acad. Sci. 328, 381–386.

Hsissou, Y., Bouchaou, L., Krimissa, M., Mudry, J., 2001. Caractérisation de l'origine de la salinité des eaux de la nappe côtière d'Agadir (Maroc). First international Conference on Salt Water and Coastal Aquifers (SWICA)-Monitoring, Modeling and Management. Essaouira, Morocco, 23–25.

IAEA//WMO, 2004. Global Network of Isotopes in Precipitation. Available from: http://isohis.iaea.org.

Koepnick, R.B., Burke, W.H., Denison, R.E., Hetherington, E.A., Nelson, H.F., Otto, J.B., Waite, L.E., 1985. Construction of the seawater 87Sr/86Sr curve for the Cenozoic and Cretaceous: supporting data. Chem. Geol. (Isotope Geosci. Section) 58, 55–81.

Korte, C., Kozur, H.W., Bruckschen, P., Veizer, J., 2003. Strontium isotope evolution of Late Permian and Triassic seawater. Geochim. Cosmochim. Acta 67, 47–62.

Krimissa, S., Michelot, J.L., Bouchaou, L., Mudry, J., Hsissou, Y., 1999. Sur l'origine par altération du substratum schisteux de la minéralisation chlorurée des eaux d'une nappe côtière sous climat semi-aride (Chtouka-Massa, Maroc). Comptes Rendus Geosci. 336, 1363–1369.

Mahlknecht, J., Garfias-Sodis, J., Tech, R.Aa., 2006. Geochemical and isotopic investigations on groundwater residence time and flow in the Independence Basin, Mexico. J. Hydrol. 324, 283–300.

Michel, R.L., 2005. Tritium in the Hydrologic Cycle. In: Isotopes in the Water Cycle: Past, Present and Future of Developing Science, IAEA, Springer, pp. 53–66.

Mook, W.G., 1980. Carbon-14 in hydrogeological studies. In: Fritz, P., Fontes, J.C. (Eds.), Handbook of Environmental Isotopes Geochemistry 1. Elsevier, Amsterdam, pp. 50–74.

Naftz, D.L., Peterman, Z.E., Spangler, L.E., 1997. Using d87SR values to identify sources of salinity to freshwater aquifer, Greater Aneth Oil Field, Utah, USA. Chem. Geol. 141, 195–209.

Négrel, Ph., Deschamps, P., 1996. Natural and anthropogenic budgets of a small watershed in the Massif Central (France): chemical and strontium isotopic characterization of water and sediments. Aqueous Geochem. 2, 1–27.

Négrel, Ph., Casanova, J., Aranyossy, J.F., 2001. Strontium isotope systematics used to detect the origin of groundwaters sampled from granitoids: the Vienne case (France). Chem. Geol. 177, 287–308.

Négrel, Ph., Petelet-Giraud, E., 2005. Strontium isotopes as tracers of groundwater-induced floods: the Somme case study (France). J. Hydrol. 305, 99–119.

Peterman, Z.E., Wallin, B., 1999. Synopsis of strontium isotope variations in groundwater at AÈspoÈ, Southern Sweden. Appl. Geochem 14, 939–951.

Plummer, L.N., 2005. Dating of young groundwater. In: handbook: Isotopes in the water cycle. Past, Present and Future of Developing Science. IAEA. Springer, 193–218.

Probst, A., El Gh'mari, A., Aubert, D., Fritz, B., McNutt, R., 2000. Strontium as a tracer of weathering processes in a silicate catchment polluted by acid atmospheric inputs, Strenbach, France. Chem. Geol. 170, 203–219.

Petalas, C.P., Diamantis, I.B., 1999. Origin and distribution of saline groundwaters in the upper Miocene aquifer system, coastal Rhodope area, northeastern Greece. Hydrogeol. J. 7, 305–316.

Richter, B.C., Kreitler, C.W., 1993. Geochemical Techniques for Identifying Sources of Ground-water Salinization. CRC Press, Boca Raton.

Risacher, F., Alonso, H., Salazar, C., 2003. The origin of brines and salts in Chilean salars: a hydrochemical review. Earth-Sci. Rev. 63, 249–293.

Roether, W., Schiltzer, R., 1991. Eastern Mediterranean deep water renewal on the basis of chlorofluoromethane and tritium data. Dynamics Atm. Oceans 15, 333–354.

Rozanski, K., Araguás-Araguás, L., Gonfiantini, R., 1993. Isotopic patters in modern global precipitation. In: Swart, P.K. et al. (Eds.), Climate Change in Continental Isotopic Records, Geophys. Monogr. Ser, vol. 78. AGU, Washington, DC, pp. 1–36.

Swarzenski, P.W., Reich, C.D., Spechler, R.M., Kindinger, J.L., Moore, W.S., 2001. Using multiple geochemical tracers to characterize the hydrogeology of the submarine spring off Crescent Beach, Florida. Chem. Geol. 179, 187–202.

Salomons, W., Mook, W.G., 1986. Isotope geochemistry of carbonates in the weathering zone. In: Fritz, P., Fontes, J.C. (Eds.), Handbook of Environmental Isotopes Geochemistry 1. Elsevier, Amsterdam, pp. 239–265.

Schlosser, P., Stute, M., Doerr, H., Sonntag, C., Munnich, K.O., 1988. Tritium/3He dating of shallow groundwater. Earth Planet. Sci. Lett. 89, 353–362.

Sivan, O., Yechieli, Y., Herut, B., Lazar, B., 2005. Geochemical evolution and timescale of seawater intrusion into the coastal aquifer of Israel Geochim. Cosmochim. Acta 69, 579–592.

Weisrock, A., 1980. Géomorphologie et paléo environnement de l'Atlas atlantique (Maroc) thèse Es-Sciences, Université de Paris I, France, 931 p.

Weisrock, A., Delibrias, G., Rognon, P., Coude-Gaussen, G., 1985. Variations climatiques et morphogenèse au Maroc atlantique (30–33°N)à la limite Pléistocène-Holocène. Bull. Soc. Geol. Fr. 8, 565–569.

Veizer, J., Compston, W., 1974. 87Sr/86Sr composition of seawater during the Phanerozoic. Geochim. Cosmochim. Acta 38, 1461–1484.

Veizer, J., Ala, D., Azmy, K., Bruckschen, P., Buhl, D., Bruhn, F., Carden, G.A.F., Diener, A., Ebneth, S., Godderis, Y., Jasper, T., Korte, C., Pawellek, F., Podlaha, O.G., Strauss, H., 1999. Sr-87/Sr-86, delta C-13 and delta O-18 evolution of Phanerozoic seawater. Chem. Geol. 161, 59–88.

Veizer, J., Buhl, D., Diener, A., Ebneth, S., Podlaha, O.G., Bruckschen, P., Jasper, T., Korte, C., Schaaf, M., Ala, D., Azmy, K., 1997. Strontium isotope stratigraphy: potential resolution and event correlation. Palaeogeogr. Palaeoclimatol. Palaeoecol. 132, 65–77.

Vengosh, A., Heumann, K.G., Juraske, S., Kasher, R., 1994. Boron isotope application for tracing sources of contamination in ground water. Environ. Sci. Technol. 28, 1968–1974.

Vengosh, A., Rosenthal, E., 1994. Saline groundwater in Israel: its bearing on the water crisis in the country. J. Hydrol. 156, 389–430.

Vengosh, A., Gert, J., De Lange, G.J., Starinsky, A., 1998. Boron isotope and geochemical evidence for the origin of Urania and Bannock brines at the eastern Mediterranean: Effect of water-rock interactions. Geochim. Cosmochim. Acta 62, 3221–3228.

Vengosh, A., Starinsky, A., Kolodny, Y., Chivas, A.R., 1991. Boron-isotope geochemistry as a tracer for the evolution of brines and associated hot springs from the dead sea, Israel. Geochim. Cosmochim. Acta 55, 1689–1695.

Vengosh, A., Starinsky, A., Kolodny, Y., Chivas, A.R., Raab, M., 1992. Boron isotope variations during evaporation of sea water: new constraints on the marine vs. nonmarine debate. Geology 20, 799–802.

Vengosh, A., 2003. Salinization and saline environments. In: Sherwood Lollar, B. (Ed.), Environmental Geochemistry, Treatise in Geochemistry, vol. 9. Elsevier Science.

Vengosh, A., Kloppmann, W., Marie, A., Livshitz, Y., Gutierrez, A., Banna, M., Guerrot, C., Pankratov, I., Ranan, H., 2005. Sources of salinity and boron in the Gaza Strip: Natural contaminant flow in the southern Mediterranean Coastal aquifer. Water Resour. Res. 41, W01013. doi:10.1029/2004WR003344.

Vengosh, A., Hening, S., Ganor, J., Mayer, B., Weyhenmeyer, C.E., Bullen, T.D., Paytan, A., 2007. New isotopic evidence for the origin of groundwater from the Nubian Sandstone Aquifer in the Negev, Israel. Appl. Geochem. 22, 1052–1073.

Vengosh, A., Gill, J., Davisson, M.L., Huddon, G.B., 2002. A multi isotope (B, Sr, O, H, C) and age dating (3H-3He, ^{14}C) study of groundwater from Salinas Valley, California: Hydrochemistry, dynamics, and contamination processes. Water Resour. Res. 38, 9-1–9-17.

Yechieli, Y., Sivan, O., Lazar, B., Vengosh, A., Ronen, D., Herut, B., 2001. Radiocarbon in seawater intruding into the Israeli Mediterranean coastal aquifer. Radiocarbon 43, 773–781.